Regenerative properties of pyramidal cell dendrites in area CA1 of the rat hippocampus

Mogens Andreasen and John D. C. Lambert*

PharmaBiotec, Institute of Physiology, University of Aarhus, DK-8000 Aarhus C, Denmark

1. Intracellular recordings were obtained from 184 distal apical dendrites and twenty-six somata of CA1 pyramidal neurones in the rat hippocampal slice preparation. In the presence of 3·25 mM K^+ 200 ms suprathreshold current pulses evoked three different types of firing patterns in the apical dendrites, all of which were distinct from regular somatic firing. Fast tetrodotoxin (TTX)-sensitive spiking was evoked in 38·8% of the dendrites. Compound spiking, consisting of an initial fast spike followed by one or more secondary slow spikes of variable amplitude and duration, was seen in 44·1% of dendrites. 'Classical' burst firing, resembling intrinsic somatic bursts, was evoked in 17·1% of the dendrites.

2. In fast spiking dendrites, the spikes evoked by long depolarizing pulses were rarely overshooting, showed prominent accommodation and declined progressively to about one-third of the initial amplitude. The amplitude of single dendritic fast spikes (50·6 ± 1·5 mV; mean ± S.E.M.) was smaller than that of somatic spikes (82·2 ± 1·9 mV) and their rate of rise (81·3 ± 4·3 V s^{-1}) was markedly slower than that of somatic spikes (291·5 ± 17·8 V s^{-1}). However, the thresholds were not significantly different (dendrites, −49·8 ± 0·8 mV; somata, −50·8 ± 1·3 mV). These results indicate that fast spikes in the distal parts of apical dendrites are generated by a local regenerative Na^+ current.

3. 4-Aminopyridine (4-AP, 0·1–0·5 mM) caused a dose-dependent slowing of the repolarization of the fast spikes, while tetraethylammonium (TEA, 2 mM) and Co^{2+} (2 mM) induced a slowing of the late phase of the repolarization. These results indicate that the transient outward K^+ current, I_A, and the Ca^{2+}-activated K^+ current, I_C, are involved in the repolarization of dendritic Na^+-dependent spikes.

4. Compound spiking was completely blocked by TTX (0·5–1 μM). The secondary slow spikes within the complex were blocked by Co^{2+} (2 mM), nifedipine (10 μM) and high concentrations (>50 μM) of verapamil, while Ni^{2+} (100–300 μM) had no effect. Thus, compound spiking consists of an initial Na^+-dependent spike followed by one or more slow Ca^{2+}-dependent spikes mediated by L-type Ca^{2+} channels located in the apical dendrites.

5. In fast spiking dendrites, 4-AP (0·5–2·5 mM) changed the firing pattern from regular fast spiking to compound spiking. In the presence of 4-AP (0·1–0·5 mM), the single fast spike evoked by a short (20 ms), threshold current pulse, was followed by secondary slow spikes of variable amplitude and duration. This suggests that activation of a dendritic I_A has a significant influence on the spatial activation of dendritic L-type Ca^{2+} channels.

6. Increasing the extracellular K^+ concentration to 5·25 mM had no effect on the passive membrane properties of the dendrites. However, the incidence of bursting dendrites increased to 83%, while the remaining 17% showed compound spiking. The burst responses were blocked by TTX (0·5–1 μM), while Ni^{2+} (100–300 μM), nifedipine (10 μM) and verapamil (50–100 μM) had no effect, indicating that neither T- nor L-type Ca^{2+} channels are involved in dendritic bursting.

* To whom correspondence should be addressed.

Synaptic excitation of hippocampal CA1 pyramidal neurones is principally mediated by CA3 pyramidal neurones, axons of which form the Schaffer collateral (ipsilateral) and commissural (contralateral) pathways. These pathways are glutamatergic, and the excitatory postsynaptic potential (EPSP) results from simultaneous activation of non-*N*-methyl-D-aspartate (NMDA) and NMDA receptors on the postsynaptic membrane (Andreasen, Lambert & Jensen, 1989). The pharmacological and kinetic properties of this glutamatergic EPSP have hitherto been mostly studied at the somatic level. However, the primary site of glutamatergic synaptic contacts is on the highly arborized dendritic tree (Andersen & Lømo, 1966). The electrical properties of the dendrites will therefore have a substantial influence on the integration and propagation of synaptic potentials. If synaptic potentials are conducted electrotonically to the soma, dendritic impedance would markedly attenuate EPSPs generated at distant synapses (Rall, 1962). Analysis of extracellular field potentials has, however, shown that EPSPs evoked at distal and proximal synapses have similar amplitude and shape indices at the somatic level (Andersen, Silfvenius, Sundberg & Sveen, 1980). It has been proposed that active electrogenesis in the dendrites amplifies the otherwise small effects of distal synapses and thereby compensates for the loss due to dendritic impedance (Spencer & Kandel, 1961; Andersen & Lømo, 1966). Support for this notion has come from analysis of extracellular field potentials and current-density profiles. These have shown that orthodromic stimulation evokes a short-duration, tetrodotoxin (TTX)-sensitive negative field potential and a current sink in the proximal dendrites, which propagates over the somatodendritic axis and precedes the somatic population spike (Andersen & Lømo, 1966; Taube & Schwartzkroin, 1988*b*; Turner, Meyers & Barker, 1989; Herreras, 1990; Turner, Meyers, Richardson & Barker, 1991). Intradendritic recordings from CA1 pyramidal neurones have provided evidence for voltage-dependent Na^+ and Ca^{2+} currents in the apical dendrites (Wong, Prince & Basbaum, 1979; Masukawa & Prince, 1984; Wong & Stewart, 1992). Activation of these currents by synaptic potentials conducting through the dendritic tree could enhance the probability of spike discharge in the initial segment.

The functional implications of active electrogenesis in the dendrites for the propagation of synaptic potentials have still to be fully resolved. Because of the mechanistic differences between non-NMDA- and NMDA-receptor-coupled ionophores (Mayer & Westbrook, 1987), it is conceivable that potentials mediated by these receptors could be influenced differentially by dendritic electrogenesis. Conduction through the NMDA-operated ionophore is regulated by Mg^{2+} in a voltage-dependent manner (Mayer & Westbrook, 1987) such that the ionophore conducts little current at normal values of resting membrane potential (V_m). NMDA receptors would not therefore be expected to make a large contribution to normal excitatory synaptic transmission. However, we have previously demonstrated that a substantial part of the EPSP recorded in the somata of CA1 pyramidal neurones at resting V_m is due to activation of NMDA receptors (Andreasen *et al.* 1989). One explanation for this apparent discrepancy could be that local interactions between synaptic potentials and voltage-dependent dendritic currents depolarize the dendritic membrane to such an extent that the voltage-dependent block of the NMDA-operated ionophore is partially relieved.

With the prime intention of investigating the kinetic properties of synaptic potentials at their site of generation and their propagation to soma, we have made intradendritic recordings from the distal third of CA1 pyramidal neurone apical dendrites. However, it soon became apparent that our results concerning the electrophysiological properties of the dendrites digressed in several respects from those reported by others (Wong *et al.* 1979; Wong & Stewart, 1992). Because these properties are clearly important for the integration and propagation of synaptic potentials, we found it necessary to analyse them thoroughly. Here we present results showing that the apical dendrites of CA1 pyramidal neurones are capable of generating several types of firing patterns. Furthermore, the results suggest that there are differences in the local distribution of transient outward K^+ currents, which to a great extent determines the excitability of the dendritic tree.

METHODS

Experiments were performed on hippocampal slices prepared from seventy-eight male Wistar rats (250–300 g). After anaesthetizing with chloroform, the rats were decapitated and the brain removed and quickly placed in a standard Ringer solution (see below) at 4 °C. The hippocampus was dissected free and slices (400 μm thick) were cut on a McIlwain tissue chopper. The slices were immediately transferred to the recording chamber, where they were placed on a nylon-mesh grid at the interface between warm (31–33 °C) standard Ringer solution (pH 7·3) and warm humidified carbogen (95% O_2–5% CO_2). Perfusion flow rate was 1 ml min^{-1}. The slices were allowed to rest for at least 1 h before recordings were started.

Intrasomatic and intradendritic recordings from CA1 pyramidal neurones were obtained using borosilicate glass microelectrodes (1·2 mm o.d., Clark Electromedical Instruments, Pangbourne, UK) filled with 4 M potassium acetate (tip resistances, 60–110 MΩ). To obtain intradendritic recordings from the distal apical dendrites of CA1 pyramidal neurones, penetrations were made at the border between stratum radiatum and stratum lacunosum-moleculare, which is easily identified in the slice preparation as a relatively abrupt shift in colour and structure

between the two strata. After each experiment the approximate location of the recording electrode was marked on a schematic diagram of the hippocampal slice for future reference.

Dendritic penetrations were accepted for analysis if the resting V_m was stable and $\geqslant -50$ mV and there was a membrane input resistance (R_{in}) of $\geqslant 10$ MΩ. Recordings usually lasted for 15–45 min, though a few penetrations lasted for >2 h. Standard intrasomatic recordings from CA1 pyramidal neurones were obtained for the purpose of comparison. The criteria for accepting somatic recordings were similar to those used earlier (Andreasen *et al.* 1989).

Conventional intracellular recording techniques were employed, using a high input impedance amplifier (Axoclamp 2A, Axon Instruments) with bridge-balance and current injection facilities. Results were digitized on-line using a Labmaster A/D converter and pCLAMP acquisition software (Axon Instruments) on a 486 PC computer and recorded for off-line analysis using a modified digital audio processor (Sony PCM-701es) and a video tape-recorder.

Values are given as means ± S.E.M. unless otherwise indicated. For statistical analysis, χ^2 and Student's t tests were used as appropriate.

Drugs and solutions

The composition of the standard Ringer solution was (mM): NaCl, 124; KCl, 3·25; NaH_2PO_4, 1·25; $NaHCO_3$, 20; $CaCl_2$, 2; $MgSO_4$, 2; D-glucose, 10; bubbled with carbogen (pH 7·3). The following modified Ringer solutions were used. (1) Co^{2+}-containing medium, in which $CaCl_2$ was replaced by 2 mM $CoCl_2$ and NaH_2PO_4 was omitted to prevent precipitation. (2) A high-K^+ medium in which 2 mM KCl was added to the standard Ringer solution to give a final K^+ concentration of 5·25 mM. (3) Ni^{2+}-containing medium, in which $NiCl_2$ was added to the standard Ringer solution to give a final concentration of 100 or 300 μM.

All pharmacological compounds were made up in aqueous stock solutions of 100–1000 times the required final concentration and diluted in the standard Ringer solution as appropriate. Nifedipine was predissolved in dimethylsulphoxide (DMSO) and the final concentration of DMSO in the perfusion medium was 0·1%. Because of its light sensitivity, all experiments with nifedipine were performed in a darkened room. All substances named in the text were purchased from Sigma (USA) with the following exceptions: DL-2-amino-5-phosphonovaleric acid (APV, Tocris Neuramin, Bristol, UK), 4-aminopyridine (4-AP, Merck, Germany), 6-cyano-7-nitroquinoxaline-2,3-dione (CNQX; a gift from Tage Honoré, Novo Nordisk, Måløv, Denmark).

Histochemistry

Cells were loaded with biocytin by passive diffusion or by applying positive current pulses (200 ms, 0·2–0·5 nA, 1 Hz) through the recording electrodes containing 2 M potassium acetate and 2% biocytin. The membrane and firing properties of the impaled dendrite were characterized either before or after active injection of biocytin. Slices were maintained in the recording chamber for 15–30 min after recording and then transferred to fixative (4% paraformaldehyde), in which they were kept for 24–48 h. For staining, the slices were first rinsed in Tris-buffered saline (TBS) containing 1% Triton X-100 (TBS-T) for 15 min, followed by 10 min in a solution consisting of 80 ml TBS plus 10 ml hydrogen peroxide (30%) and 10 ml methanol to block endogenous peroxidase activity. After rinsing with TBS-T for 3 × 15 min, the slices were incubated for 2 h with avidin–peroxidase, diluted 1 : 70 in TBS-T. After two rinses of 15 min with TBS, the avidin-bound peroxidase was visualized by incubation for 2 min with 50 mg diaminobenzidine dissolved in 100 ml TBS to which 0·03 ml hydrogen peroxide was added immediately before use. The slices were finally mounted with Eukit and inspected with bright-field microscopy. Preparations were photographed, and selected neurones were drawn using camera lucida (e.g. Fig. 1).

RESULTS

Identification of intradendritic recordings

The data presented here are based on 184 intradendritic recordings (of which 30 were biocytin filled) and twenty-six intrasomatic recordings from CA1 pyramidal neurones that fulfilled the criteria given in Methods. The intradendritic recordings were obtained from the distal third of the apical dendrites (300–400 μm from stratum pyramidalis). In all cases, the somata of these biocytin-labelled neurones were located in or near stratum pyramidalis and the morphology of the cells was characteristic of pyramidal neurones (Fig. 1*A*) thereby confirming the intradendritic nature of the recordings. In some cases, a small swelling could be seen in one of the first-order branches of the apical dendrites corresponding to the location of the recording site. The rest of the recordings (154) were identified as intradendritic on the basis of the location of the recording site and the similarity of the electrophysiological properties to those obtained from histochemically verified intradendritic recordings (Fig. 1*Ba*), which differed unambiguously from those of CA1 pyramidal cell somata. Occasionally recordings were obtained from presumed interneurones located in or near stratum lacunosum-moleculare (Lacaille & Schwartzkroin, 1988), an example of which is shown in Fig. 1*A*. These recordings were clearly distinguishable from intradendritic recordings (Fig. 1). The fast spikes evoked in interneurones were all overshooting and of the same amplitude and were always followed by a fast and a slow after-hyperpolarization (AHP) (Fig. 1*Ca*). In contrast, the spikes evoked in the distal apical dendrites varied greatly in amplitude, were seldom overshooting and repolarized to baseline with no evidence of an AHP (Fig. 1*Ba*). The R_{in} of interneurones was 62 ± 14·9 MΩ ($n = 8$), which was nearly three times that of dendrites (see below) and the current–voltage (I–V) relationship of interneurones showed a more pronounced inward rectification (compare Fig. 1*Bb* and *Cb*).

The passive membrane properties of distal apical dendrites

The resting V_m of the distal apical dendrites was −64·7 ± 0·3 mV (range, −72 to −55 mV; $n = 150$) which was not significantly different ($P > 0·02$) from that found

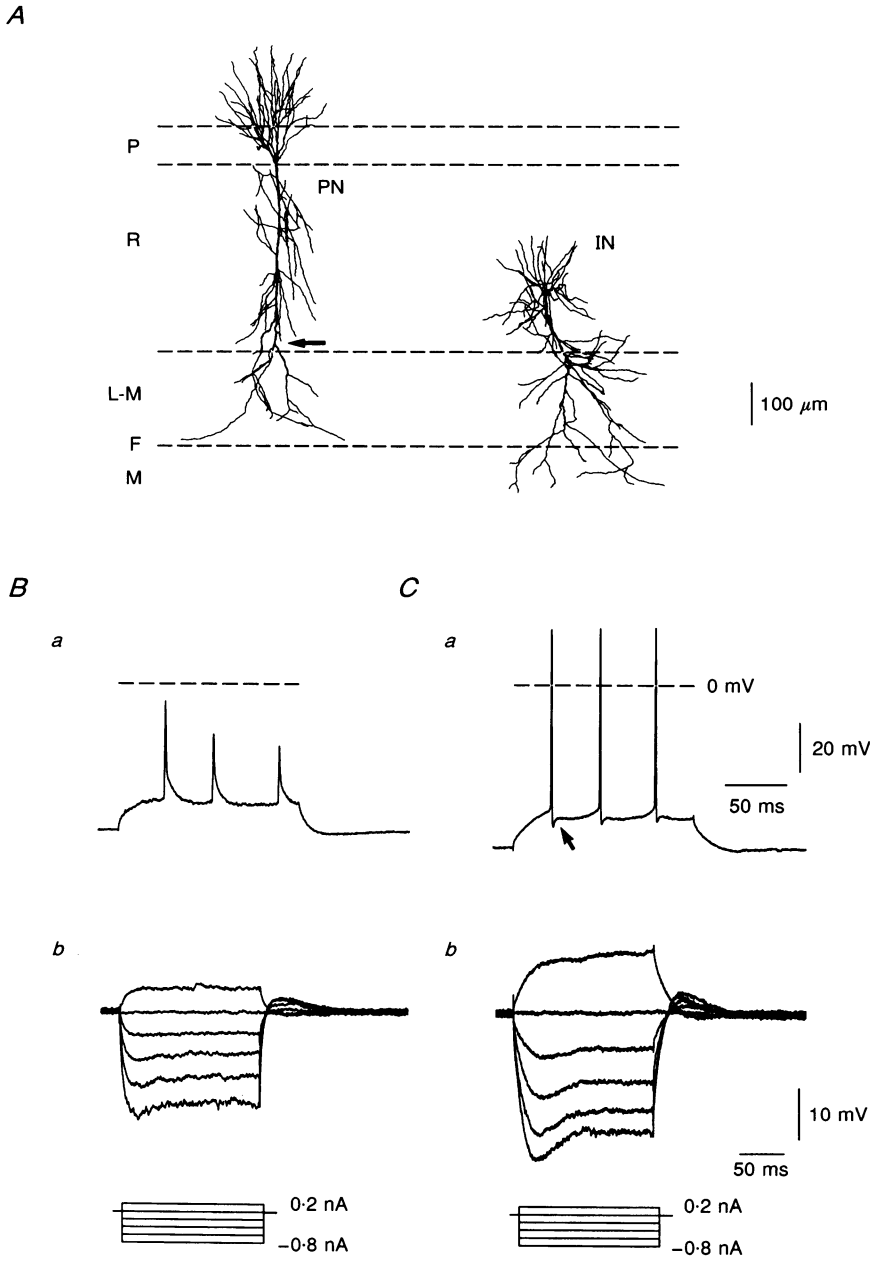

Figure 1. Electrophysiological and morphological properties of neurones recorded near the border of the stratum lacunosum-moleculare in the hippocampal slice

A, camera lucida drawings of a biocytin-loaded CA1 pyramidal neurone (PN) filled through an intradendritic recording and a biocytin-filled interneurone (IN) located in the distal stratum radiatum (R) and stratum lacunosum-moleculare (L-M). Note that the dendrites of the interneurone extend across the hippocampal fissure (F). The approximate site of the penetration is indicated by the arrow. P, stratum pyramidalis; M, stratum moleculare. *B*, electrophysiological responses obtained with the intradendritic recording from the pyramidal neurone shown in *A*. A suprathreshold depolarizing current pulse (+0·4 nA) evoked repetitive firing of fast spikes (*a*), which did not overshoot and progressively decreased in amplitude. Note the very broad base of the spikes with little evidence of an AHP. The *I–V* relationship of the dendrite (*b*) shows inward rectification, which develops with larger hyperpolarizing current pulses. *C*, electrophysiological properties of the interneurone shown in *A*. A suprathreshold depolarizing current pulse (+0·3 nA) (*a*) evoked repetitive firing of fast, overshooting spikes that were followed by a fast and medium AHP (arrow). The *I–V* relationship (*b*) showed marked inward rectification with both hyperpolarizing and depolarizing current pulses. The dashed lines indicate zero membrane potential. Resting V_m: *B*, −61 mV; *C*, −68 mV.

in intrasomatic recordings (−66·3 ± 0·7 mV; range −75 to −60 mV; $n = 26$), and within the range reported by other investigators for more proximal dendritic levels (see Discussion). R_{in} and the membrane time constant τ_m were determined from the response to a small (to minimize contamination by voltage-dependent membrane currents) 150 ms hyperpolarizing current pulse. To calculate R_{in}, the change in V_m at the end of the voltage transient was measured. The R_{in} for distal dendrites was 21·1 ± 0·6 MΩ (range, 12–41 MΩ; $n = 150$), which was significantly smaller ($P < 0·001$) than that for somata (38 ± 3·1 MΩ; range, 22–75 MΩ; $n = 26$).

The I–V relationship was examined by injection of hyperpolarizing and depolarizing current pulses (range, −0·8–0·3 nA). The records in Fig. 2 are from two different pyramidal neurones selected on the basis of similar values of resting V_m and R_{in} to facilitate comparison of the dendritic and somatic responses. During injection of hyperpolarizing currents in the dendrite, V_m reached an initial peak value within 20–30 ms and then decayed ('sagged') slowly towards Resting V_m (Figs 1*Bb* and 2*Aa*). This depolarizing sag, which was present in 57% (49/70) of the intradendritic recordings examined, developed at around −70 mV and increased in size with further hyperpolarization, though it varied considerably in amplitude between individual recordings. When the current pulse was terminated, V_m exhibited a transient depolarizing overshoot, the size of which was proportional to the amount of sag which developed during the current pulse. The recordings from the somata were qualitatively similar to those from the dendrites (Fig. 2*Ba*). When measured as the peak change in V_m, the I–V relationship for both dendrites and somata was linear (Fig. 2). However, when

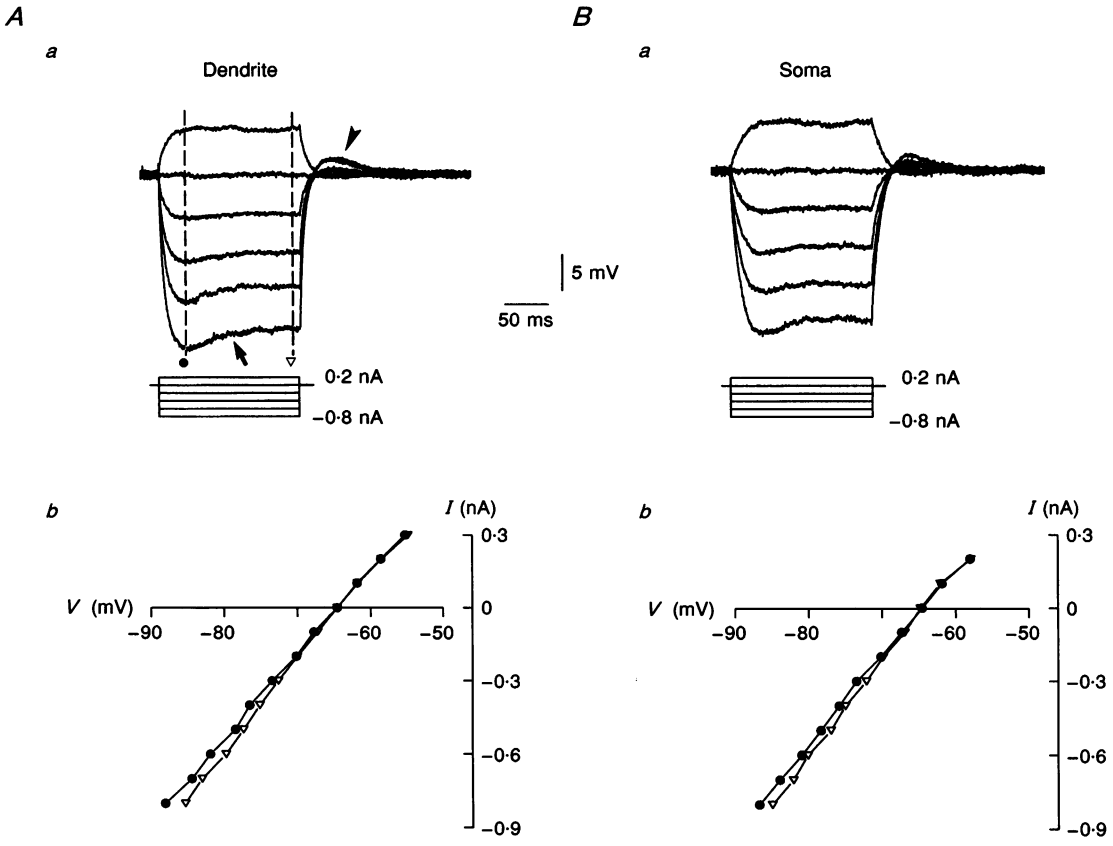

Figure 2. Current–voltage relationships of the somatic and dendritic membranes

Aa, responses of an apical dendrite to positive and negative current pulses. When hyperpolarized to about −70 mV, a depolarizing 'sag' (arrow) became evident which grew in amplitude with increasing hyperpolarization. When the negative current pulses were turned off, there was a transient depolarization (arrowhead) before the potential returned to resting V_m. *Ab*, plot of the I–V relationship for the dendrite in *Aa*. The voltage was measured at the peak (●) and at the end (plateau; ▽) of the electrotonic pulses, as indicated by the dashed lines above. The I–V relationship of the peak responses was nearly linear, while the relationship for plateau responses showed slight inward rectification. *B*, a somatic recording selected with similar values of resting V_m and R_{in} for comparison with *A*. The I–V relationship and rectification are very similar to those of the dendrite. Resting V_m: *A*, −64 mV; *B*, −64·5 mV. R_{in}: *A*, 26·2 MΩ; *B*, 26·8 MΩ.

measured at the end of the current pulse, the I–V relationship was non-linear at potentials more negative than −70 mV, resulting in an increase in slope conductance characteristic of inward rectification. On average, inward rectification in the dendrites became evident between −75 and −65 mV ($n = 49$). Similar inward rectification has been described in intrasomatic recordings from CA1 pyramidal neurones (Fig. 2; Halliwell & Adams, 1982; Segal & Barker, 1984) and has been attributed to a non-inactivating mixed cation current, termed I_Q.

τ_m was determined by fitting the time course of the initial potential change induced by a small hyperpolarizing current pulse. The time course was well described by a single exponential function in both dendrites ($r^2 > 0{\cdot}96$) and somata ($r^2 > 0{\cdot}99$). The τ_m for the dendritic membrane (4·9 ± 0·22 ms, $n = 39$) was significantly faster ($P < 0{\cdot}001$) than for the somatic membrane (15 ± 2·02 ms, $n = 9$).

Regenerative properties of distal apical dendrites

In somatic recordings, depolarizing current pulses (200 ms) to above firing threshold evoked regular firing of high amplitude spikes (Fig. 4*A*). In contrast, three different firing patterns were evoked in the apical dendrites (Fig. 3*A*), each of which was clearly distinct from that seen in somatic recordings. The first type consists of regular firing of fast spikes of variable amplitude and at variable frequency (Fig. 3*A a*). In the following this will be termed fast spiking (where the term

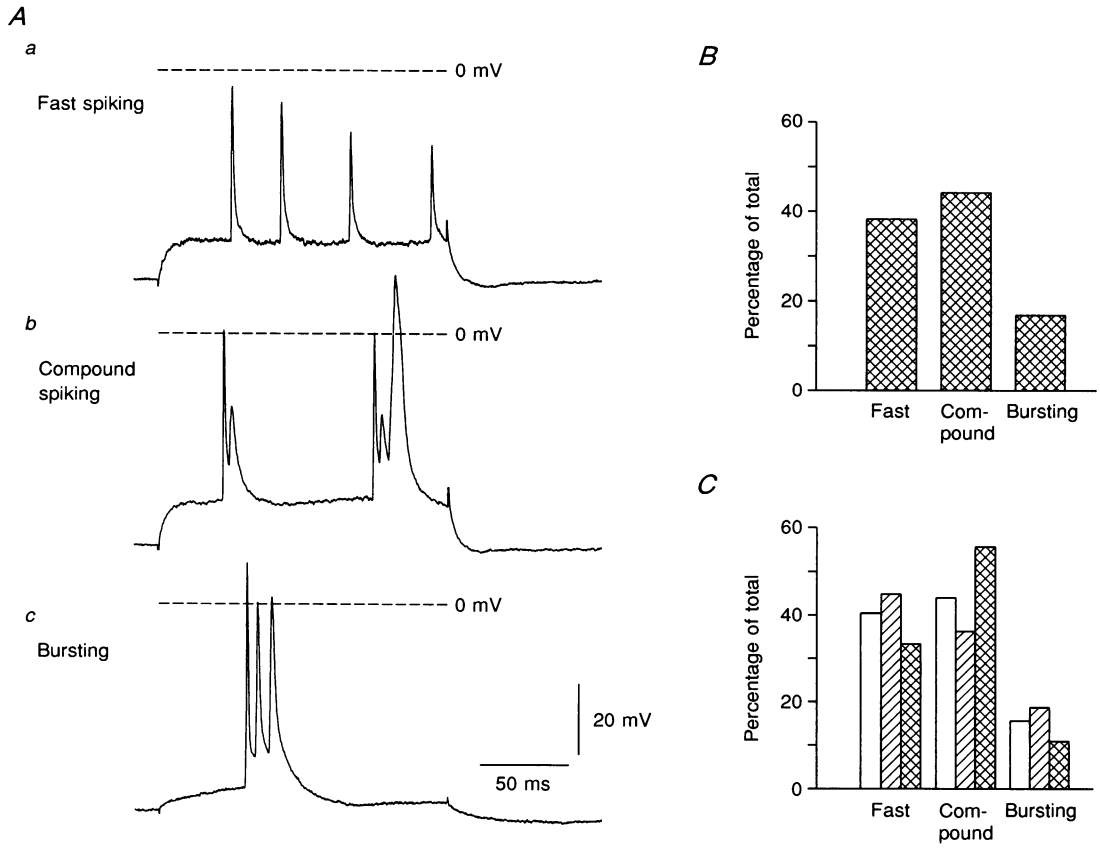

Figure 3. Dendritic firing patterns and their incidence in apical dendrites

A, representative examples of the three types of firing patterns evoked in distal apical dendrites by 200 ms suprathreshold current pulses. *A a*, fast spiking activity; the spikes accommodated and declined progressively in amplitude. *A b*, compound spiking, consisting of an initial fast spike followed by one or two secondary spikes of variable amplitude and duration. *A c*, 'classical' burst response, consisting of several fast spikes surmounting a slow depolarizing potential. The dashed lines indicate zero membrane potential. Resting V_m: *A a*, −69·5 mV; *A b*, −70·3 mV; *A c*, −69 mV. *B*, histogram of 152 intradendritic recordings. Fast spiking (Fast) occurred in 38·8%, compound spiking (Compound) in 44·1% and 'classical' burst firing (Bursting) in 17·1% of the dendritic recordings. *C*, distribution of the firing patterns in relation to the hippocampal level from which the slices were prepared. □, total; ▨, septal; ▩, temporal. 139 of the slices could be clearly identified as originating from the septal or temporal pole. The overall distribution of firing patterns was similar to that seen in *B*. A χ^2 test showed no significant correlation between the incidence of the firing patterns and the location along the longitudinal axis of the hippocampus.

'fast' relates to the rate of rise and half-width of the dendritic spikes). The second type showed burst-like responses, consisting of an initial fast spike followed by one or more secondary slow spikes of variable amplitude and duration (Fig. 3*A b*). These secondary spikes often had distinct inflexions on the rising and/or falling phase (e.g. Figs 8*Ba* and *D* and 9). Due to the complex nature of this burst-like response, and also to distinguish it from the third type of response, this type of firing pattern is termed compound spiking. The third type consisted of a cluster of fast spikes riding on a depolarizing envelope (Fig. 3*A c*). This resembles burst responses occasionally seen in somatic recordings and is therefore referred to as a 'classical' burst. A more detailed description of the individual firing patterns and their responses to pharmacological manipulations is given in the following sections.

On the basis of the firing patterns evoked by 200 ms long suprathreshold current pulses in control conditions, each of 152 intradendritic recordings could be allocated to one of three subgroups (Fig. 3*B*). In 38·8% (59/152) of the recordings only fast spiking could be evoked, irrespective of the intensity of the pulse. In 44·1% (67/152) compound spiking was seen, either as the sole firing pattern or together with fast spiking. In the remaining 17·1% (36/152) of the intradendritic recordings only 'classical' burst firing was evoked. Since the threshold response of these dendrites to a short depolarization consisted of a

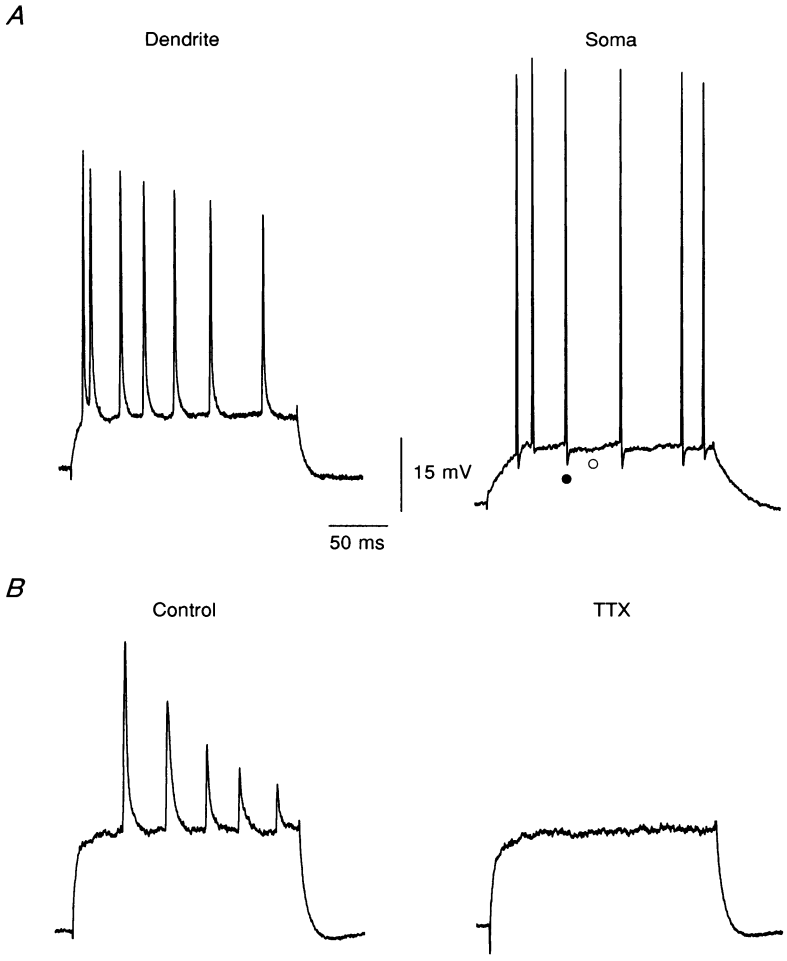

Figure 4. Dendritic fast spikes are different from somatic spikes

A, typical responses of a fast spiking apical dendrite and a soma to a 200 ms depolarizing current pulse (+0·5 and +0·7 nA, respectively). Although repetitive firing of fast spikes was evoked in both instances, there were several differences. The peak amplitude of the somatic spikes was considerably larger than that of the dendritic spikes. The amplitude of somatic spikes was relatively constant, while the dendritic spikes declined progressively. Somatic spikes were followed by a fast (●) and a medium (○) AHP, while the dendritic spikes all decayed to baseline with no evidence of an AHP. The duration at the base of the spike was therefore considerably longer in dendrites than in the somata. *B*, TTX (1 μM) completely blocked the dendritic fast spikes. Resting V_m: *A*, dendrite, −63 mV; *A*, soma, −70 mV; *B*, −64·5 mV.

burst of spikes which outlasted the duration of the pulse, these dendrites will be referred to as intrinsic bursters. As will be shown later, changes in the extracellular K^+ concentration ($[K^+]_o$) or blockade of certain K^+ currents leads to changes in the distribution of dendritic firing patterns, indicating that the regenerative properties of the apical dendrites are labile.

Area CA1 can be subdivided into CA1a, CA1b and CA1c, within which somatic recordings indicate differences in the distribution of regular fast spiking and intrinsic bursting pyramidal neurones (Masukawa, Benardo & Prince, 1982). No such subfield-dependent differences in the distribution of the three dendritic firing patterns were found. We also investigated the distribution of the aforementioned firing patterns in slices taken from the septal and temporal poles of the hippocampus. Of 152 recordings, eighty-five were obtained from septal slices and fifty-four from temporal slices. Although fast spiking was slightly more frequent in septal slices and compound spiking more frequent in temporal slices (Fig. 3*C*), a χ^2 test revealed that the differences were not statistically significant ($0{\cdot}05 < P < 0{\cdot}10$).

Fast spikes

The following describes results from dendrites in which only fast spiking could be evoked, although the kinetic properties of individual fast spikes evoked in compound spiking dendrites were similar. When the distal dendrites were depolarized to above firing threshold with long-duration (200 ms) current pulses, several fast spikes were evoked (Figs 1*Ba*, 3*Aa* and 4*A*). These were clearly distinct from fast spikes evoked at the somatic level (Fig. 4*A*) or in interneurones (Fig. 1*Ca*), one major difference being that, when several spikes were evoked, there was a progressive fall in the amplitude of the spikes in the dendrites (Fig. 4*A* and *B*), but not in the somata (Fig. 4*A*) or interneurones (Fig. 1*Ca*). With 200 ms current pulses, the decrease in amplitude of dendritic spikes could be more or less pronounced (compare Fig. 4*A* with 4*B*). However, when longer current pulses (900 ms) were used, the amplitude of the fast spikes usually decreased to a stable level of about one-third of the amplitude of the first fast spike evoked (not shown). A more elaborate description of this phenomenon will be presented elsewhere (M. Andreasen & J. D. C. Lambert, unpublished observations). The dendritic spikes usually peaked at or below 0 mV (Figs 1*Ba*, 3*Aa* and 4*A*) and were only rarely observed to overshoot, while somatic and interneuronal spikes always showed substantial overshoots (Figs 1*Ca* and 4*A*). Dendritic fast spikes were completely blocked by TTX (0·5–1 μM; Fig. 4*B*) implying that they are generated by a regenerative Na^+ current.

Using short (10–20 ms) depolarizing current pulses of increasing amplitude, the mean threshold for evoking dendritic fast spikes was found to be $-49{\cdot}8 \pm 0{\cdot}8$ mV ($n = 25$), which was not significantly different ($P < 0{\cdot}5$) from somatic fast spikes ($-50{\cdot}8 \pm 1{\cdot}3$ mV, $n = 17$). At threshold, one or two high amplitude fast spikes were evoked in the dendrites (Fig. 5*Aa*) with a peak amplitude (measured from the base of the spike) of $50{\cdot}6 \pm 1{\cdot}5$ mV (range, 38–65 mV; $n = 25$) and a rate of rise of $81{\cdot}3 \pm 4{\cdot}3$ V s^{-1}. For comparison, threshold-evoked somatic spikes (Fig. 5*Ba*) had a mean peak amplitude of $82{\cdot}2 \pm 1{\cdot}9$ mV ($n = 17$) and a rate of rise of $291{\cdot}5 \pm 17{\cdot}8$ V s^{-1} ($n = 17$). The repolarizing phase of the dendritic spikes also differed markedly from that of somatic spikes (Fig. 4*A*). As previously documented, somatic spikes in CA1 pyramidal neurones are usually followed by a fast and a medium AHP (Fig. 4*A*). In contrast, dendritic fast spikes were followed by a depolarizing after-potential (DAP) with no indication of an AHP (Figs 1*Ba*, 3*Aa*, 4*A* and 4*B*). Thus, dendritic fast spikes evoked at threshold were markedly broader at the base, even though their half-width ($1{\cdot}2 \pm 0{\cdot}04$ ms) was very similar to that of somatic spikes ($0{\cdot}98 \pm 0{\cdot}02$ ms). The repolarization of dendritic fast spikes with an amplitude $\geqslant 40$ mV ($n = 41$), was best described by a double exponential function with time constants of $0{\cdot}96 \pm 0{\cdot}07$ and $5{\cdot}77 \pm 0{\cdot}3$ ms. Even though dendritic fast spikes were not followed by an AHP, prominent spike accommodation was still evident in most recordings (e.g. Figs 3*Aa* and 4*A*).

When the current intensity of short depolarizing pulses was increased further above that required to evoke firing, the second dendritic spike became slower (mean rate of rise 49 ± 4 V s^{-1}; $n = 17$) and broader (half-width, $1{\cdot}87 \pm 0{\cdot}1$ ms) and its amplitude decreased to $37{\cdot}2 \pm 1{\cdot}1$ mV. In twelve of seventeen dendrites tested, a further increase in current intensity elicited a third spike which was even slower (rate of rise $30{\cdot}8 \pm 3{\cdot}5$ V s^{-1}; half-width, $3{\cdot}28 \pm 0{\cdot}4$ ms) than the second spike. Although it varied greatly in amplitude, it was usually larger than the preceding spike (Fig. 5*A b*). Increasing the current amplitude did not have the same dramatic effects on the kinetics of somatic spikes. There was a slight broadening of the secondary spikes together with a decline in the AHP and a slight decrease in amplitude (Fig. 5*B b*). Note that even though the AHP declined, the somatic spikes repolarized to a more negative value than the pre-spike potential. In contrast, dendritic spikes repolarized to a progressively more depolarized level (Fig. 5*A b*).

Several outward K^+ currents have been shown to be involved in the repolarization of somatic spikes in CA1 pyramidal neurones (for review see Storm (1990)). We investigated the possible role of these in the repolarization of spikes in dendrites in which only fast spikes could be evoked. We first examined the effect of 4-AP, which blocks the transient K^+ current, I_A, and the slowly inactivating

K^+ current, I_D, in hippocampal neurones (Storm, 1990) and slows the repolarization of somatic spikes (Storm, 1987). In control conditions, the amplitude of a short-duration (20 ms) current pulse was adjusted to evoke a single fast spike just following termination of the current injection, thereby avoiding interference by the capacitance transient. In these, and the later experiments with TEA, glutamatergic and $GABA_A$ receptor-mediated synaptic inputs were blocked by using a mixture of CNQX (10 μM), APV (50 μM) and bicuculline (10 μM). Low concentrations (50 μM) of 4-AP had no effect on the spike. In three of the four dendrites tested, increasing the concentration of 4-AP to 0·1 mM resulted in the appearance of a second low amplitude, slow spike (Fig. 6*A*). This arose from the DAP, which itself had become more pronounced and appeared at a more positive potential. Increasing the concentration of 4-AP further to 0·5 mM ($n = 4$) resulted either in the appearance of a third high amplitude spike with a very slow time course (Fig. 6*A*), or in a more complex secondary component with multiple peaks similar to that seen in Fig. 6*C* and *D*. A further increase in the amplitude of the DAP was also seen, as shown in Fig. 6*B*, where the initial fast spikes are shown superimposed on an expanded time scale. The kinetics of the initial fast spike were also changed, with a concentration-dependent increase in the time to peak and a slowing of the repolarization (Fig. 6*B*). At present, we have no explanation for the 4-AP-induced slowing of the rising phase. When 200 ms current pulses were used, 10–20 min perfusion with 0·5 mM 4-AP changed the firing pattern from fast spiking to compound

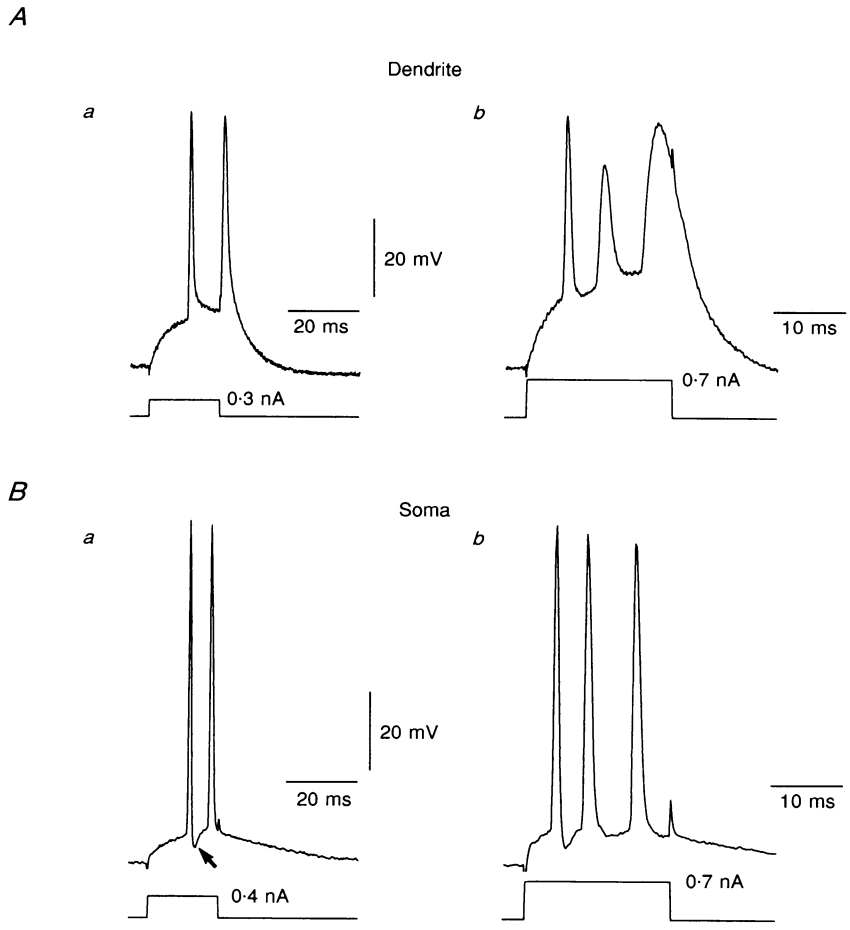

Figure 5. Firing properties of fast spiking dendrites and somata

A, response of a dendrite to a short (20 ms) current pulse which depolarized the membrane to the threshold for firing (*a*) and suprathreshold levels (*b*). At threshold (+0·3 nA), two fast spikes were evoked, the second being somewhat broader than the first. With suprathreshold stimulation (+0·7 nA) (*b*), the initial fast spike was followed by two spikes of variable amplitude and slower time course. *B*, at threshold (+0·4 nA) two spikes of similar amplitude were evoked in a soma (*a*). In contrast to the dendrite, the first somatic spike was followed by a fast AHP (arrow). With suprathreshold stimulation (+0·7 nA), three spikes were evoked which decreased slightly in amplitude. A slight broadening of the spikes and decline in the AHP were also evident here. Resting V_m: *A*, −63 mV; *B*, −70 mV.

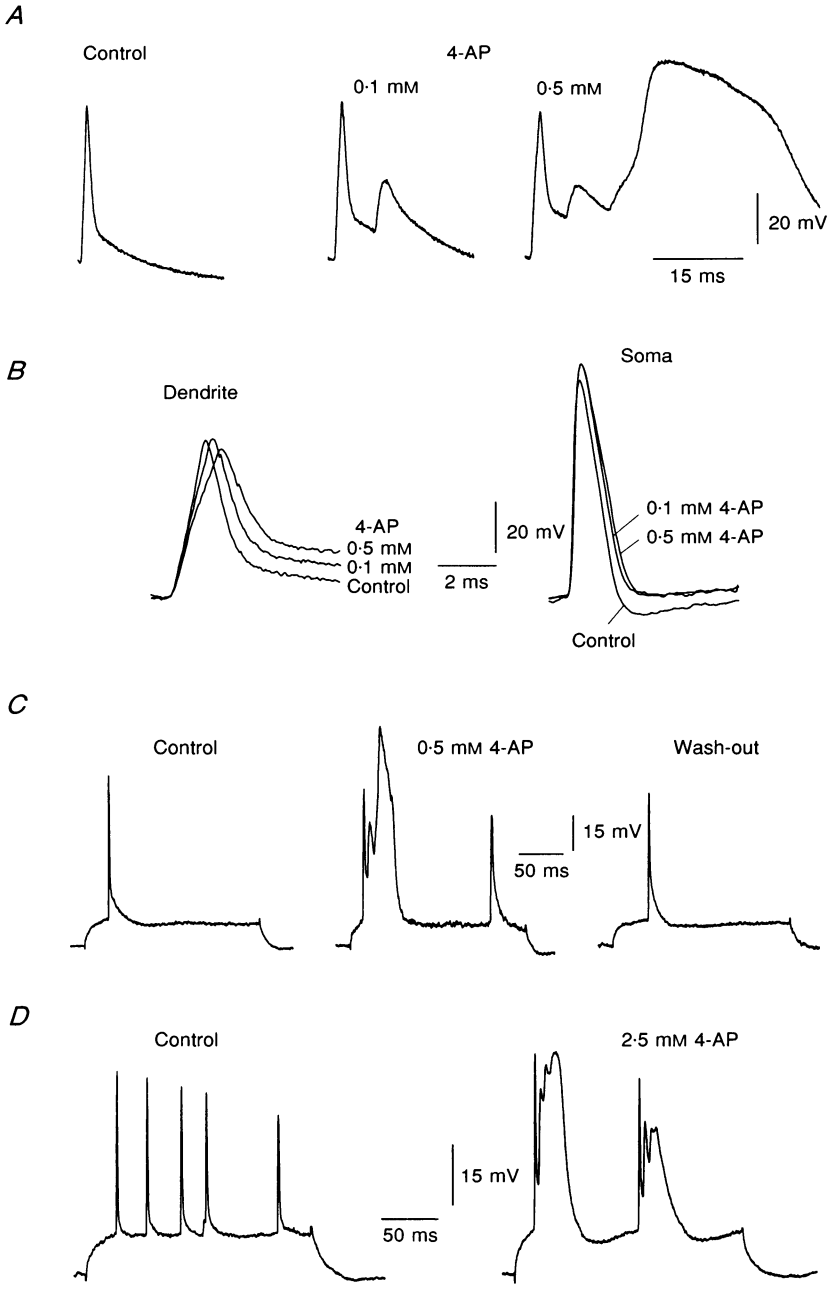

Figure 6. The effect of 4-AP on dendritic firing properties

Experiments were performed in the presence of CNQX (10 μM), DL-APV (50 μM) and bicuculline (10 μM). All recordings were obtained from apical dendrites in which only fast spiking could be evoked. *A*, the intensity of a 10 ms depolarizing current pulse (not shown) was adjusted to evoke a fast spike on the decaying phase of the voltage transient. In the presence of 0·1 mM 4-AP, the amplitude of the DAP increased and a second low amplitude spike appeared. In 0·5 mM 4-AP, the amplitude of the DAP increased further and a third very prolonged spike of high amplitude appeared. *B*, the effects of 4-AP on dendritic (left) and somatic (right) fast spikes. The dendritic spikes are the initial fast spikes in *A* superimposed on an expanded time scale. The concentration-dependent increase in the amplitude of the DAP is clearly evident. 0·1 mM 4-AP increased the amplitude of somatic spikes slightly and slowed the repolarization in a uniform manner. Little additional effect was obtained on increasing the concentration of 4-AP to 0·5 mM. *C*, 4-AP (0·5 mM) changed the dendritic response to a 200 ms current pulse (+0·5 nA) from regular fast spiking to compound spiking. This effect was reversed after 20 min wash-out. *D*, a similar transition in firing pattern was obtained using a 5 times higher concentration of 4-AP in another neurone. Resting V_m: *A*, −60 mV; *B* (soma), −68 mV; *C*, −72 mV; *D*, −69 mV.

spiking (Fig. 6*C*; $n = 4$). This effect of 4-AP was reversed after 20 min wash-out. No additional effects were seen on increasing the concentration of 4-AP to 2·5 mM (Fig. 6*D*, $n = 5$).

By way of reference, we also tested the effect of 4-AP on the somatic spikes ($n = 3$). The effect of 4-AP was near maximum at 0·1 mM, where it caused an increase in amplitude and a general broadening of the spike with no change in time to peak (Fig. 6*B*). These effects have been described previously by Storm (1987) and have been attributed to a block of I_A, indicating that the effects of 4-AP on the single fast spikes and firing patterns in dendrites are not due to a non-selective block of a delayed rectifying K^+ current.

The transient Ca^{2+}-activated K^+ current (I_C) has also been shown to be involved in the repolarization of somatic spikes (Storm, 1987). I_C is blocked by low concentrations (1–2 mM) of TEA, which induced a concentration-dependent slowing of the latter part of the somatic spikes, giving the appearance of a shoulder on the repolarizing phase (Fig. 7*A*). With 2 mM TEA, a small increase in amplitude was also occasionally seen (Fig. 7*A*). In the apical dendrites, TEA also induced a slowing of the repolarizing phase of the fast spike, with the later part being mostly affected (Fig. 7*B*). Because of its Ca^{2+} dependency, I_C is eliminated in Ca^{2+}-free medium or by inorganic Ca^{2+} channel blockers. Perfusion of a medium in which Ca^{2+} had been replaced by Co^{2+} for 20–30 min resulted in a slowing of the repolarization of dendritic fast spikes with a marked broadening at the base (Fig. 7*C*; $n = 3$).

Compound spiking

Although the overall composition of compound spiking varied greatly (Figs 8*A* and *B* and 9), some common features were evident. Compound spiking was always prefaced by a single fast spike (Figs 8 and 9) followed at variable latency by one or more secondary slow spikes. Often, only one secondary spike was seen, arising from the DAP following the fast spike (Figs 8*A* and *C* and 9*B*). The amplitude of the second spike was usually about half that of the fast spike, although it could sometimes be of high amplitude (Fig. 9*C*). A third high amplitude slow spike was occasionally evoked, which arose on the falling phase of the second spike at a variable latency. In some instances, the second spike was almost completely embedded in the third spike and was only evident as a small inflection on the rising phase of the third spike (Fig. 8*Ba*). Several individual peaks were often seen near the top and during the decay of the third spike, indicating multiple spiking (Figs 8*Ba* and 9*A*). In some cases, a given constant-current pulse evoked compound spiking consisting of a fast spike followed by one or two slow spikes (Fig. 8*A*), while in others an increase in current amplitude was necessary to elicit more than one slow spike.

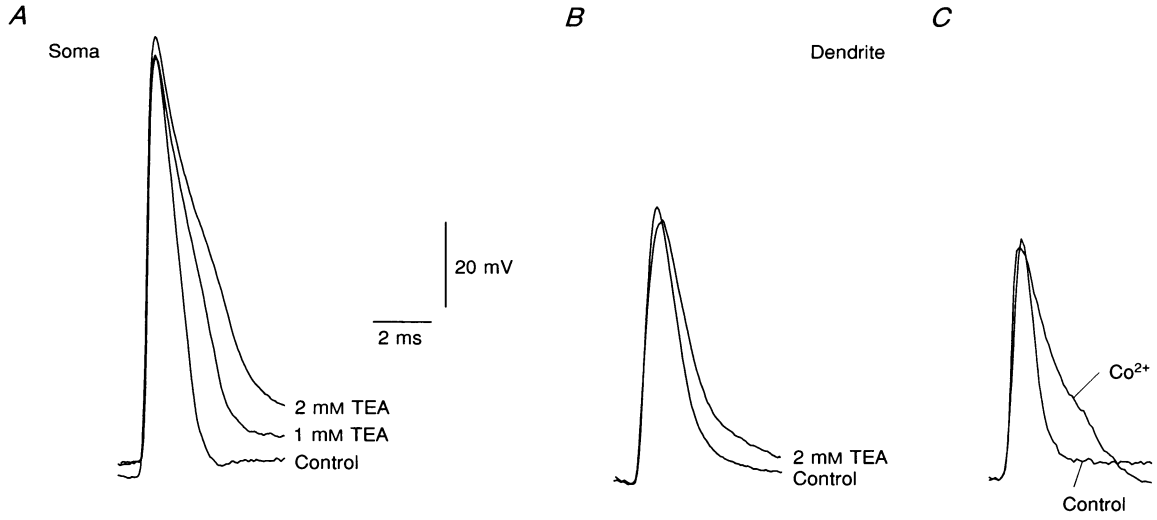

Figure 7. The effect of TEA on the repolarization of somatic and dendritic spikes

Experiments were performed in the presence of CNQX (10 μM), DL-APV (50 μM) and bicuculline (10 μM). The recordings were obtained from apical dendrites in which only fast spiking could be evoked. All spikes were evoked by a 10 ms depolarizing pulse, adjusted in strength to evoke a spike just after the end of the pulse. *A*, the repolarization of the somatic spike was slowed by TEA in a concentration-dependent manner. The late phase of the repolarization was mostly affected resulting in the appearance of a shoulder. 2 mM TEA also caused a slight increase in the amplitude of the spike. *B*, TEA caused a similar, though less pronounced, delay in the repolarization of the dendritic fast spikes. *C*, Co^{2+}-containing medium also induced a broadening of the dendritic fast spikes. Resting V_m: *A*, −66 mV; *B*, −70 mV; *C*, −68 mV.

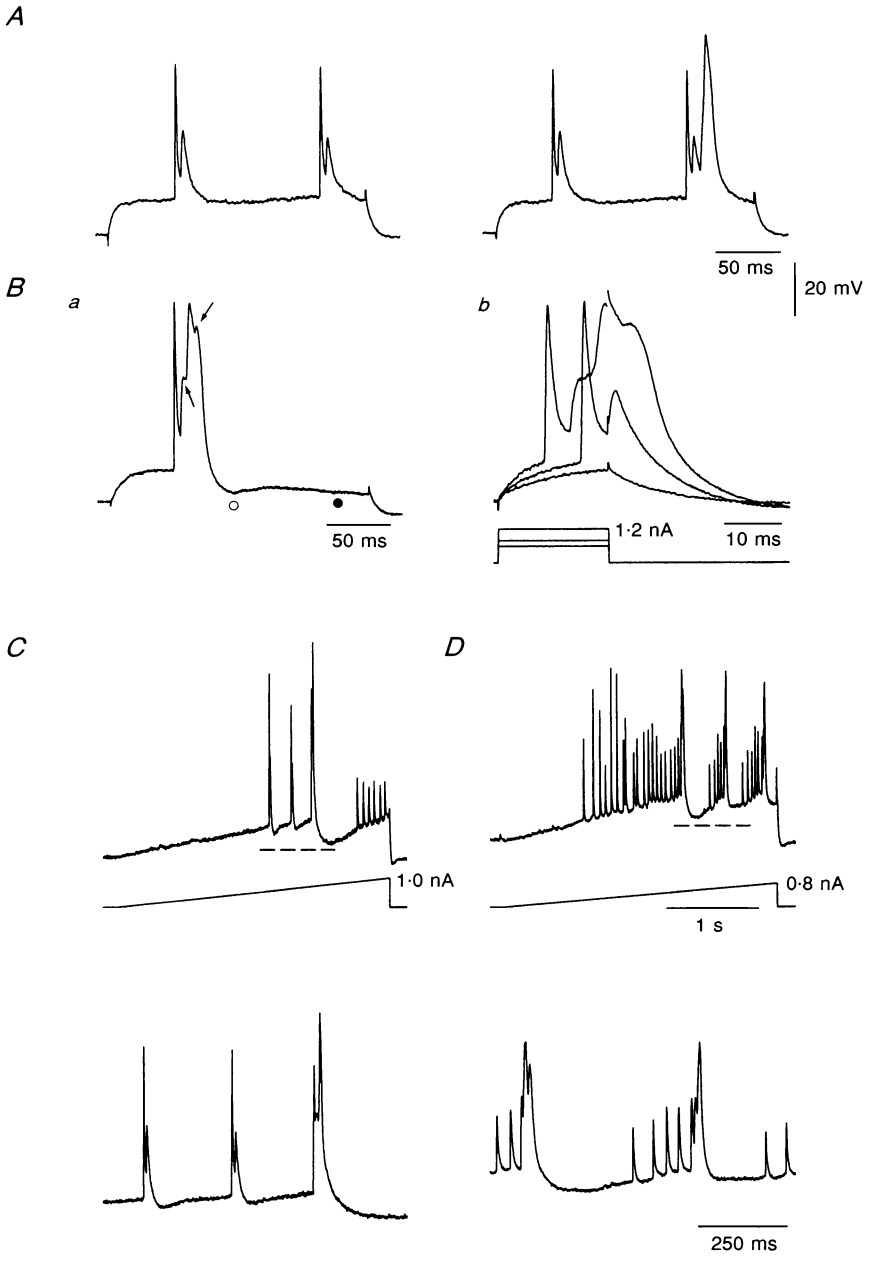

Figure 8. Compound spiking in apical dendrites

A, example of two types of compound spiking recorded in the same apical dendrite with the same current pulse (+0·7 nA). *B*, example of compound spiking in another dendrite. *a*, the initial fast spike was followed by a very broad, high amplitude slow spike on which several smaller peaks were discernible (arrows). Compound spiking was often followed by a relatively fast AHP (○), and occasionally by a very slow AHP (●). *b*, response of the same dendrite to injection of 20 ms depolarizing pulses of increasing amplitude. The threshold response consisted of an initial fast spike followed by a second, low amplitude spike. When the current strength was increased, the latency of the first spike became shorter and the overall response became similar to that shown in *a*. *C* and *D*, slow (3 s) current ramps evoked two types of responses in compound spiking dendrites. *C*, in most dendrites repetitive compound spiking was evoked, occasionally followed by repetitive firing of small fast spikes. *D*, in a minority of neurones, repetitive firing of fast spikes preceded compound spiking. The period indicated by the dashed line in *C* and *D* above is shown below on an expanded time scale. Resting V_m: *A*, −71 mV; *B*, −65·6 mV; *C*, −70 mV; *D*, −63·5 mV.

The threshold response of most (67%) of the dendrites with compound spiking consisted of a fast spike followed by a low amplitude, broader spike (Fig. 8*Bb*) with a mean threshold of $-54{\cdot}6 \pm 1{\cdot}1$ mV ($n = 14$), which was significantly ($P < 0{\cdot}005$) more negative than the threshold for spikes in fast spiking dendrites. In the remaining 33% of compound spiking dendrites, the threshold response was a single fast spike with a threshold similar to that found in fast spiking dendrites. The threshold for evoking compound spikes in these dendrites was $-45{\cdot}2 \pm 1{\cdot}6$ mV ($n = 7$). Fig. 8*D* shows an example of the response of such a dendrite to the injection of a current ramp, which evoked repetitive firing of fast spikes followed by compound spiking. In contrast to single fast spikes, compound spiking was often followed by a more or less pronounced AHP (Figs 8*Ba*, *C* and *D* and 9). The size of the AHP was positively correlated to the total area of the secondary slow component (Fig. 8*C*). When the fast spike was followed by a low amplitude slow spike, the AHP was small. However, when a third spike or a high amplitude second spike was evoked, a very marked AHP was seen (Figs 8*C* and 9*C*). The AHP following a large secondary component usually consisted of an initial relatively fast AHP, followed by a slow, more prolonged AHP (Fig. 8*Ba*).

Compound spiking was completely blocked by TTX (0·5–1 μM; $n = 5$; Fig. 9*A*) and no activity could be evoked by increasing the current intensity. On replacing Ca^{2+} in the perfusion medium with Co^{2+} ($n = 7$), the secondary spikes were blocked leaving fast spikes, which fired at a higher frequency (Fig. 9*B*). The organic Ca^{2+}

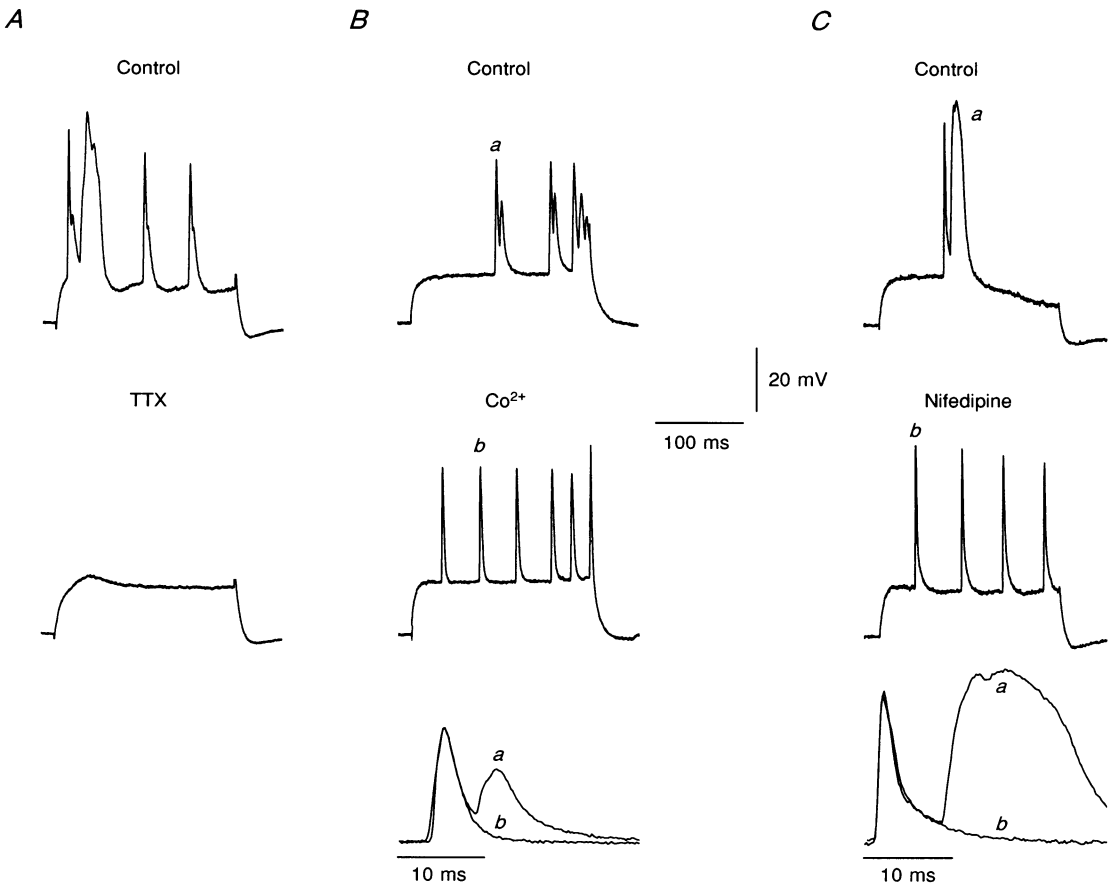

Figure 9. Compound spiking consists of two components

A, compound spiking was completely blocked by TTX (1 μM). *B*, perfusion with medium containing 2 mM Co^{2+} blocked the secondary slow spikes and increased the frequency of fast spiking. The spikes marked *a* and *b* are shown below superimposed on an expanded time scale, where it is seen that the secondary spikes were blocked by Co^{2+} with no change in the amplitude or kinetics of the initial fast spike. *C*, nifedipine (10 μM) also blocked the secondary slow spikes, while the initial fast spike was unchanged (spikes *a* and *b* superimposed below). As with Co^{2+}, fast spikes were evoked at a higher frequency. However, in contrast to Co^{2+}, the spikes were followed by a small AHP. Resting V_m: *A*, −65 mV; *B*, −60 mV; *C*, −63 mV.

channel blocker, nifedipine (10 μM), also blocked the secondary slow spikes ($n = 5$) (Fig. 9*C*), whereafter there was an increase in the frequency of single fast spikes. In two experiments, the secondary spikes were blocked within 4–5 min, at which time the concentration of nifedipine within the slices would not have reached equilibrium, indicating that the effective concentration was substantially lower than 10 μM. Another Ca^{2+} channel blocker, verapamil, in concentrations up to 50 μM, had no effect on compound spiking. At 100 μM, however, verapamil also blocked the secondary component of compound spiking leaving the fast spikes ($n = 3$).

Ni^{2+} in low concentrations is a relatively specific blocker of low threshold T-type Ca^{2+} channels (Fox, Nowycky & Tsien, 1987). Ni^{2+} (100–300 μM) had no effect on the secondary components of compound spiking ($n = 3$), suggesting that T-type Ca^{2+} channels are not activated during the secondary spikes.

Burst firing

Firing in intrinsic bursting dendrites consisted of a cluster of two or three fast spikes riding on a depolarizing envelope, followed by a more or less pronounced AHP (Fig. 10*A a*). The amplitude of the second spike was always smaller than the first, whereas the amplitude of the third spike varied to a great extent (Figs 3*Ac* and 10) and could be the same size (though never larger) as the first fast spike. A progressive increase in spike duration was also seen, with the third spike having a duration of 8–10 ms at the base.

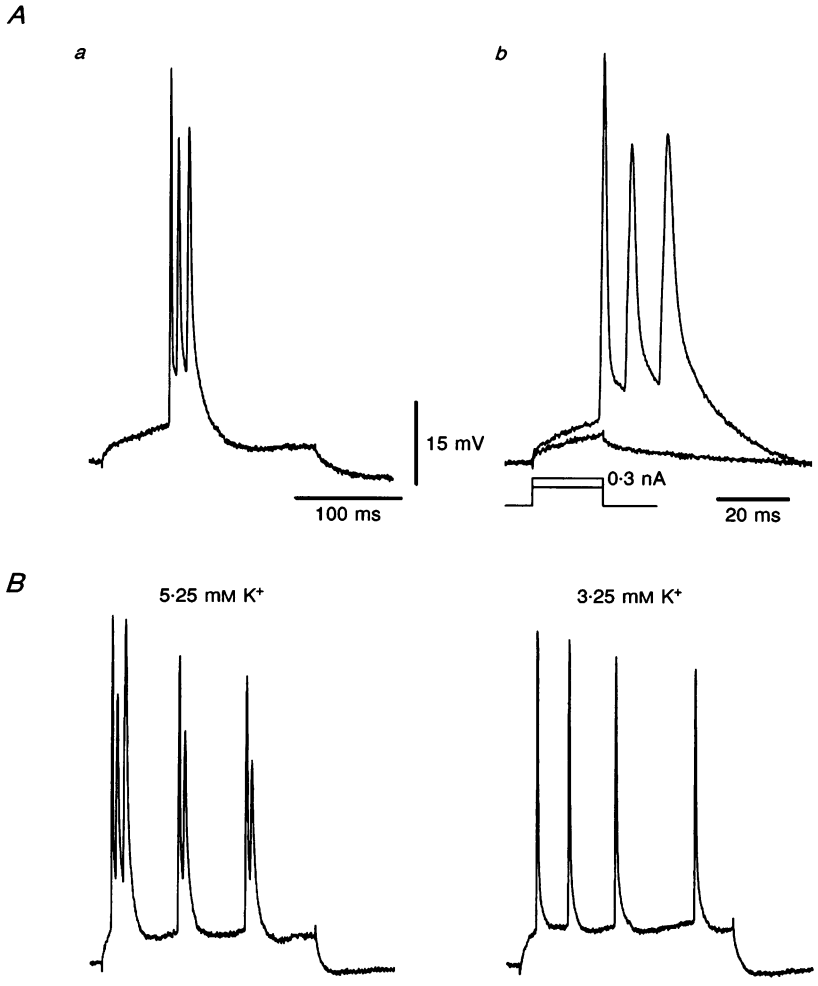

Figure 10. 'Classical' burst firing in apical dendrites

A, 'classical' burst responses evoked in an apical dendrite in a standard medium containing 3·25 mM K^+. *a*, the burst elicited by a 200 ms depolarizing pulse (+0·2 nA) consisted of three fast spikes riding on a depolarizing envelope followed by an AHP. *b*, burst evoked at threshold (0·3 nA) by a short-duration (20 ms) current pulse. The burst was elicited just before termination of the current pulse, which it outlasted. *B*, the effect of extracellular K^+ on burst firing. In 5·25 mM K^+ several bursts were evoked by a 200 ms current pulse (+0·5 nA). *b*, 23 min after lowering $[K^+]_o$ to 3·25 mM, the same pulse evoked single fast spikes followed by small AHPs. Resting V_m: *A*, −69 mV; *B*, −62·5 mV in 5·25 mM K^+ and −63·8 mV in 3·25 mM K^+.

Since our study was conducted in 3·25 mM K^+, which is lower than most previous investigations (Table 1), it was relevant to examine how changes in $[K^+]_o$ affect the firing properties of the distal apical dendrites. In the following experiments, the slices were perfused for at least 45 min with a medium containing 5·25 mM K^+, before starting to record. In this medium, the incidence of 'classical' bursting dendrites was 83% (19/23), which compared with 17% in 3·25 mM K^+, while in the remaining 17% compound spiking was evoked. The configuration and composition of the burst recorded in 5·25 mM K^+ is similar to that recorded in intrinsic bursting dendrites in 3·25 mM K^+ (Fig. 10B). The increase in $[K^+]_o$ had no significant effect on the passive membrane properties of the dendrites (resting V_m, −62·2 ± 1·5 mV; R_{in}, 19·2 ± 1·9 MΩ, $n = 17$).

Because these recordings started in 5·25 mM K^+ it is possible that these dendrites would have been intrinsic bursters in 3·25 mM K^+. However, in four experiments, $[K^+]_o$ was reduced to 3·25 mM and after 20–30 min perfusion the firing properties of the dendrites had changed from 'classical' bursting to fast spiking (Fig. 10*B*). This indicates that the increase in the incidence of 'classical' bursting dendrites is related to the increase in $[K^+]_o$.

Perfusion with TTX (0·5–1 μM) completely blocked the 'classical' burst responses evoked in 5·25 mM K^+ (Fig. 11*A*) and a substantial increase in current intensity evoked a broad, slowly rising spike, resembling a somatic Ca^{2+}-dependent spike (Fig. 11*B*) (Schwartzkroin & Slawsky, 1977). This spike, however, inactivated very quickly, as shown in Fig. 11*B*, where current pulses were injected at a frequency of 0·33 Hz. The first pulse (●) evoked two components, but already with the third pulse (○) the relatively fast component was absent and only a slow, very prolonged potential remained.

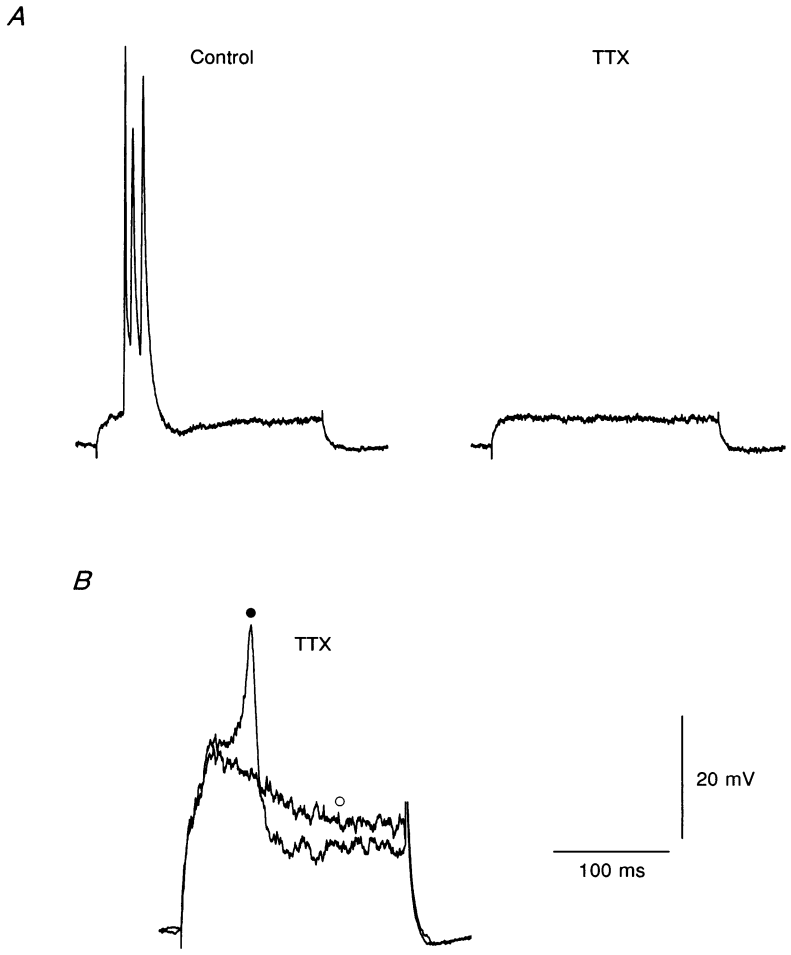

Figure 11. Effect of TTX on 'classical' bursting activity in dendrites

A, the burst activity evoked by a 0·2 nA depolarizing pulse in the presence of 5·25 mM K^+ was completely blocked by TTX (1 μM). *B*, in the presence of TTX, Ca^{2+}-dependent spikes could be evoked by a sevenfold increase in pulse strength (from 0·2 to 1·4 nA). The stimulating frequency was 0·33 Hz and the response to the first pulse (●) was a low amplitude spike followed by an AHP. This is superimposed on the response evoked by the third pulse (○), where the spike was inactivated leaving a slowly decaying potential. Resting V_m, −64 mV.

Table 1. Electrophysiological parameters of apical dendrites

Resting V_m (mV)	R_{in} (MΩ)	Spike (mV)	$[K^+]_o$ (mM)	Recording site* (μm)	Reference
> −50	48·6 ± 11·6	52·5 ± 10·2	6·25	> 150	Wong *et al.* (1979)
−59·6 ± 4·7	33·6 ± 12·7	66·6 ± 8·1	6·25	100–300	Bernado *et al.* (1982)
−62·2 ± 1·5	19·2 ± 1·9		5·25	> 350	Present study
> −55	> 30		5·0	> 100	Masukawa & Prince (1984)
−67·0 ± 0·8	50·0 ± 2	62·0 ± 1·1	5·0	250–400	Lacaille & Schwartzkroin (1988)
−55 to −65	33·0 ± 8·8	30–40	5·0	100–200	Taube & Schwartzkroin (1988)
−64.4 ± 0·5	28·5 ± 1·2		3·75	< 265	Turner *et al.* (1991)
−64·7 ± 0·3	21·1 ± 0·6	50·6 ± 1·5	3·25	> 350	Present study
−66·3 ± 0·7	38·0 ± 3·1	82·2 ± 1·9	3·25	0†	Present study

V_m, membrane potential; R_{in}, membrane input resistance; Spike, amplitude of TTX-sensitive fast spikes; * distance from stratum pyramidalis; † data from intrasomatic recordings.

Ni^{2+} (100–300 μM), nifedipine (10 μM) and verapamil (50–100 μM) had no effect on 'classical' burst firing (not shown), which suggests that neither T- nor L-type Ca^{2+} channels are involved in bursting activity in the dendrites. Although we cannot exclude the involvement of other types of Ca^{2+} channels, the high threshold for activation of Ca^{2+} spikes in the presence of TTX and their apparent rapid inactivation seem to speak against this.

DISCUSSION

Sodium-dependent spike generation in apical dendrites

Previous recordings from apical dendrites in *in vitro* preparations have shown that direct current injection or synaptic stimulation can evoke fast spikes (Wong *et al.* 1979; Benardo, Masukawa & Prince, 1982; Masukawa & Prince, 1984). These fast spikes are blocked by TTX (Wong *et al.* 1979) or QX 314 (Benardo *et al.* 1982), showing that they are due to activation of voltage-dependent Na^+ conductances. Our data confirm and extend these findings by showing that TTX-sensitive fast spikes can be recorded in the distal extremities of the CA1 apical dendrites. The important question arises as to whether Na^+-dependent dendritic spikes are generated locally or at the somatic level and then propagate passively into the apical dendrites. Spencer & Kandel (1961) originally proposed that the fast pre-potentials recorded in the somata of CA1 pyramidal neurones originated in the dendrites from one or more 'hot spots' containing a high density of voltage-dependent Na^+ channels. Subsequent analyses have shown that orthodromic stimulation evokes a TTX-sensitive negative field potential and current sink in the proximal third of the apical dendrites, which propagate towards stratum pyramidalis and contributes to the generation of the somatic population spike (Andersen & Lømo, 1966; Taube & Schwartzkroin, 1988*b*; Turner *et al.* 1989; Herreras, 1990). The primary site for spike discharge in response to synaptic inputs could therefore reside in the proximal apical dendrites. However, there is still some controversy as to whether EPSPs trigger spike generation in the proximal dendrites, or only in the initial segment. Intracellular recordings have indicated that a greater level of synaptic depolarization is required to evoke spike discharge in the proximal dendrites than in the soma (Turner *et al.* 1991). In the present study, TTX-sensitive spikes were recorded ⩾ 350 μm from the cell body. Their amplitude (50 mV) is similar to that found in proximal apical dendrites (see Table 1) and indicates that the area from which spikes can be generated extends more distally than hitherto inferred (Taube & Schwartzkroin, 1988*b*; Turner *et al.* 1989; Herreras, 1990; Turner *et al.* 1991). Even though CA1 pyramidal neurones are considered to be electrotonically compact, the high amplitude of dendritic spikes, together with the fact that they can be evoked with short (10–20 ms) current pulses, make it unlikely that they are electrotonically propagated somatic spikes (the average amplitude of which is 82·2 mV). In support of this, the threshold for generation of fast spikes is similar in the soma and the distal dendrites. Moreover, antidromic spikes (both in the presence and absence of synaptic transmission) have a peak amplitude of 15–20 mV in the distal dendrites (M. Andreasen & J. D. C. Lambert, unpublished observation; Wong & Stewart, 1992). This is consonant with an attenuation of 70–80%, indicating that the recording site is located at an electrotonic length > 1·0 from the soma. Taken together, these observations can only be reconciled if fast spikes are generated locally on the dendritic membrane. The similar thresholds for spike generation in the soma and dendrites indicates that the density of voltage-dependent Na^+ channels in the two regions are similar, as has been shown for neocortical pyramidal neurones (Stuart & Sakmann, 1994).

Taube & Schwartzkroin (1988*a*) have shown that orthodromically activated fast and slow inhibitory postsynaptic potentials (IPSP) can be recorded in the proximal apical dendrites. These IPSPs exert a depressant effect on the excitability of the dendritic tree (Wong &

Prince, 1979; Masukawa & Prince, 1984) and might explain why others have found that generation of orthodromically evoked Na^+-dependent spikes is limited to proximal apical dendrites (Taube & Schwartzkroin, 1988*b*; Turner *et al.* 1989; Herreras, 1990; Turner *et al.* 1991; Jaffe, Johnston, Lasser-Ross, Lisman, Miyakawa & Ross, 1992). Stimulation in stratum radiatum activates both excitatory and inhibitory synapses and activity of the latter could mask more distal trigger zones. These would, however, be evident when the dendritic membrane is stimulated directly, as in the present study. The concept of more distally located trigger zones is also supported by studies showing that fast Na^+-dependent spikes can be evoked in isolated apical dendrites (Benardo *et al.* 1982; Masukawa & Prince, 1984) where the proximal 100–150 μm of the dendritic tree has been removed.

The variability in amplitude of threshold Na^+-dependent spikes could have several explanations. The recording sites could be located at variable distances from the trigger zones and the fast spikes attenuated to a corresponding extent by passive filtering, or it could reflect differences in the density of Na^+ channels in the distal part of the dendritic tree. While we cannot distinguish between these possibilities, the slower rate of rise of dendritic spikes compared with somatic spikes could indicate that some degree of filtering has occurred.

The dendritic fast spikes were followed by a DAP (Figs 1, 3 and 4), which contrasts with somatic spikes (Fig. 4) and spikes recorded in presumed interneurones (Fig. 1), which were followed by a fast and a medium AHP. The initial phase of the repolarization of dendritic fast spikes had a time constant which was shorter than τ_m, indicating that an active process is involved, while the late phase was slower, with a time constant (5·77 ms) similar to τ_m, inferring that the appearance of a DAP is due to a passive repolarization of the membrane. Somatic fast spikes have also been shown to be followed by a DAP (Schwartzkroin, 1975) which has been shown to be Ca^{2+} dependent (Wong & Prince, 1981), though a non-inactivating Na^+ conductance might also be involved (Konnerth, Lux & Heinemann, 1986). It cannot, therefore, be excluded that the DAP following dendritic fast spikes is mediated by an active inward Na^+ and/or Ca^{2+} current.

In addition to the rapid initial repolarization of the fast spikes, there are several other indications that outward K^+ currents are involved in the repolarization of dendritic fast spikes. When several spikes were evoked by a suprathreshold short-duration current pulse, there was a progressive increase in the duration of the spikes (Fig. 5). This could reflect a cumulative inactivation of K^+ currents which had been activated during the initial fast spike. Most dendrites showed prominent spike accommodation (Figs 3 and 4), which has been attributed to different types of K^+ currents (Storm, 1990). The repolarization of somatic spikes in CA1 pyramidal neurones has been attributed to the activation of various outward K^+ currents: I_A, I_C and I_D (for review, see Storm, 1990). The present data suggest that similar restorative K^+ currents are present in the dendritic membrane. 4-AP induced a concentration-dependent broadening of the dendritic spikes and increased the DAP (Fig. 6). In hippocampal neurones, I_D is blocked at low (micromolar) concentrations, while I_A is blocked at high (millimolar) concentrations of 4-AP (Storm, 1990). Since low concentrations of 4-AP had no effect on the spike, it seems that I_A is predominantly involved in the repolarization of dendritic fast spikes, although a contribution from I_D cannot be definitively excluded. Immunohistochemical studies have recently shown that A-type K^+ channels are present in area CA1 with the highest density in stratum oriens and stratum radiatum, corresponding to the dendritic regions (Sheng, Tsaur, Jan & Jan, 1992).

The last two-thirds of the dendritic spike repolarization was slowed by Co^{2+} (Fig. 7) and by TEA at concentrations which would be expected to block I_C but not the delayed rectifying K^+ current (Fig. 7). This is similar to the effect of Co^{2+} and TEA on somatic spikes (Storm, 1987) and indicates that the fast spike activates I_C, which is responsible for at least the last two-thirds of the spike repolarization.

The present results therefore provide evidence that similar mechanisms are responsible for repolarization following Na^+-dependent spikes in the apical dendrites and the somata of CA1 pyramidal neurones.

Calcium-dependent spike generation in apical dendrites

Slow dendritic spikes have been described previously in hippocampal neurones (Wong *et al.* 1979; Benardo *et al.* 1982), cerebellar Purkinje cells (Llinás & Sugimori, 1980) and neocortical pyramidal cells (Amitai, Friedman, Connors & Gutnick, 1993). Partly on the basis of their resistance to TTX, these spikes have been inferred to be Ca^{2+} dependent and the present results provide direct evidence for this. Co^{2+} completely blocked the slow spikes and isolated the fast Na^+-dependent spikes (Fig. 9). Since Ca^{2+}-dependent spikes are only seen in somatic recording when several K^+ currents have been blocked, the most plausible explanation is that the Ca^{2+}-dependent spikes are generated locally in the dendrites, as suggested by other investigators (Wong *et al.* 1979; Llinás & Sugimori, 1980; Benardo *et al.* 1982; Masukawa & Prince, 1982; Amitai *et al.* 1993). This is supported by recent measurements with intracellular Ca^{2+}-sensitive indicators, which have shown that active Ca^{2+} currents are distributed throughout the apical dendrites of CA1 pyramidal neurones (Regehr & Tank, 1992; Jaffe *et al.* 1992). The AHP following compound spiking is then most likely to be due to activation of one or more types of Ca^{2+}-activated K^+ current, which is consistent with the clear relationship between the amplitude and duration of the

AHP and the total area of the Ca^{2+}-dependent spikes activated during compound spiking (Fig. 8).

Results using Ca^{2+}-sensitive indicators have shown moreover that Na^+-dependent spikes contribute significantly to the spatial activation of Ca^{2+} conductances (Jaffe *et al.* 1992; Regehr & Tank, 1992). We found further support for this interaction, in that the slow Ca^{2+}-dependent spikes were always preceded by a fast Na^+-dependent spike (Figs 8 and 9) and compound spiking was completely blocked by TTX (Fig. 9), following which Ca^{2+}-dependent spikes could not be evoked. The activation of the underlying Ca^{2+} current therefore seems to require a fast depolarization to near zero level. At least three types of voltage-activated Ca^{2+} channels have been described in CA1 pyramidal neurones: a low-threshold or T-type channel and two high-threshold channels generally termed L- and N-types (Fisher, Gray & Johnston, 1990). The requirement for a fast and relatively large depolarization indicates that high-threshold Ca^{2+} channels are responsible for the Ca^{2+}-dependent dendritic spike. In support of this are the results obtained with different organic and inorganic Ca^{2+} channel blockers. Nifedipine (10 μM) and verapamil (100 μM) completely blocked the Ca^{2+}-dependent spikes, indicating that the current is carried by L-type Ca^{2+} channels (Fox *et al.* 1987; Spedding & Paoletti, 1992). However, the relatively high concentrations of organic Ca^{2+} channel blockers used here raises the question of selectivity. High concentrations (>10 μM) of dihydropyridines may have a non-specific effect on N-type channels and reduce Na^+ and K^+ currents (Regan, Sah & Bean, 1991). Since nifedipine did not block Na^+-dependent spikes (Fig. 9), its action is at least restricted to Ca^{2+} channels. In several experiments, however, the slow dendritic spikes were blocked within 4–5 min, at which time the concentration of nifedipine in the slices would not have reached equilibrium. Thus, the effect of nifedipine was achieved with concentrations substantially lower than 10 μM, making it less likely that N-type channels are involved. In cultured hippocampal neurones, 100 μM verapamil suppresses both low- and high-threshold Ca^{2+} currents (Yaari, Hamon & Lux, 1987). The slow dendritic spikes were not affected by low concentrations of Ni^{2+}, making it unlikely that low-threshold T-type Ca^{2+} channels participate (Fox *et al.* 1987), and strongly suggesting that the effect of verapamil is due to a blockade of high-threshold L-type Ca^{2+} channels. We therefore suggest that slow dendritic spikes are mediated by currents through L-type Ca^{2+} channels, which are activated by the fast depolarization induced by the preceding Na^+-dependent spike. Yaari *et al.* (1987) have previously proposed that high-threshold Ca^{2+} channels are located predominantly in the dendrites of CA1 pyramidal neurones and receptor binding studies have shown that L-type Ca^{2+} channels are found in the dendritic field of CA1 (Jones, Kunze & Angelides, 1989; Westenbroek, Ahlijanian & Catterall, 1990). These studies moreover show that the channels are localized in high density clusters, where they may form 'hot spots', in which the density of channels is high enough to support spike generation. The appearance of several slow spikes and multiple peaks on the rising phase of individual spikes (Figs 8 and 9) could therefore be due to the generation of Ca^{2+} spikes at several distinct trigger zones in the dendrites. The variable latency between the fast spike and the following Ca^{2+} spikes indicates furthermore that the fast spike propagates variable distances before it triggers a Ca^{2+}-dependent spike. The substantial variation in amplitude of the Ca^{2+}-dependent spikes (Figs 8 and 9) could then be due to differences in the density of channels within a given 'hot spot', or it could reflect temporal summation of individual Ca^{2+} spikes which are triggered at various distances from the recording site.

Outward K^+ currents modulate the excitability of apical dendrites

Burst firing has been suggested to be the predominant response of apical dendrites of CA1 pyramidal neurones (Wong *et al.* 1979; Wong & Prince, 1979; Masukawa & Prince, 1984; Wong & Stewart, 1992) and neocortical neurones (Amitai *et al.* 1993) to depolarization. These bursts consist of several fast spikes of variable amplitude, riding on a slow depolarizing envelope, which has been proposed to be Ca^{2+} dependent. The results presented here, however, show that the apical dendrites display a much more versatile firing behaviour. The three firing patterns described are all clearly distinct from the regular firing evoked in somatic recordings. In many respects, these patterns also differ from the dendritic activity described by others, which is a combination of compound spiking and 'classical' burst firing. One explanation for this apparent discrepancy could be the different concentrations of K^+ in the extracellular medium. We used 3·25 mM K^+, which is within the range of what is considered to be the normal concentration of K^+ in the cerebrospinal fluid (Fisher, Pedley, Moody & Prince, 1976; Somjen, 1979), while in the other studies $[K^+]_o$ was between 5 and 6·25 mM (see Table 1). Our results show that changes in $[K^+]_o$ have a marked effect on the firing properties of the apical dendrites (Fig. 10). Increasing $[K^+]_o$ to 5·25 mM had no significant effect on the passive membrane properties of the apical dendrites (Table 1), but resulted in a substantial increase in the incidence of 'classical' bursting dendrites (from 17% in 3·25 mM K^+ to 83% in 5·25 mM K^+). Moreover, lowering $[K^+]_o$ from 5·25 to 3·25 mM converted 'classical' burst firing to fast spiking (Fig. 10). Besides providing an explanation for the difference between our results and those of other investigators, this marked effect of a relatively small change in $[K^+]_o$ also suggests that K^+ conductances play a

significant role in controlling the excitability of the apical dendrites.

The frequency of intrinsic bursting dendrites (17%) is similar to that reported from somatic recordings of pyramidal neurones in area CA1b of the hippocampus (Masukawa *et al.* 1982). Even though no correlation between intrinsic bursting and the different subfields in CA1 was found, these data seem to indicate that the intrinsic bursting properties of a small population of CA1 pyramidal neurones is not limited to the somatic region, but extends into the apical dendrites.

As described above, nifedipine, verapamil and Ni^{2+} had no effect on 'classical' burst firing, indicating that at least T- and L-type Ca^{2+} channels are not activated during a 'classical' burst. TTX, on the other hand, completely blocked the bursts (Fig. 11). It has been suggested that a Na^{+}-dependent mechanism is capable of generating somatic bursts (Konnerth *et al.* 1986) and, with the above reservations, our results support the role of a similar mechanism in burst generation in the apical dendrites.

In control conditions, regular fast spiking and compound spiking dendrites occurred with nearly the same frequency, and were not related to the CA1 subfields or the location within the longitudinal axis of the hippocampus (Fig. 3). These firing patterns could again represent two distinct groups of pyramidal neurones with different densities of high-threshold Ca^{2+} channels, with the highest density in compound spiking dendrites. Although this hypothesis is attractive, it is unlikely for several reasons given below. Instead, we propose that both compound spiking and regular fast spiking can be generated in dendrites of the same neurone, but that differences in the distribution of transient outward K^{+} currents determine the firing pattern in response to direct stimulation. This hypothesis is supported by the following observations. In dendrites in which a 200 ms depolarizing pulse only evoked fast spiking, short depolarizations to above spike threshold evoked an initial fast spike followed by two slow spikes of increasing duration and variable amplitudes (Fig. 5). Moreover, in control conditions, the second spike repolarized to a more depolarized level than the initial fast spike (Fig. 5), indicating a progressive increase in the amplitude of the DAP. In contrast, when several somatic spikes were evoked, each of them repolarized to nearly the same level (Fig. 5). Furthermore, we have shown above that at least I_A and I_C are involved in the repolarization of dendritic fast spikes. The threshold for activation of I_A is about −60 mV, and I_A will, therefore, be activated during the initial fast spike and will peak during repolarization of the spike, following which it will inactivate with a time constant of 15–50 ms (Storm, 1990). Steady-state inactivation of I_A is complete at potentials positive to −50 mV and hyperpolarization of the membrane is therefore required before I_A can be reactivated. Since the dendritic fast spike is not followed by any marked AHP, a substantial part of I_A will stay in the inactivated state. This will result in a broadening of the following spike and an increase in the amplitude of the DAP.

Application of 4-AP had a profound effect on the firing properties of the dendrites. Regular fast spiking in control medium was transformed into compound spiking in the presence of 4-AP and, as predicted above, the amplitude of the DAP was increased (Fig. 6), which provides strong support for the proposed involvement of I_A. It implies furthermore that the difference in firing behaviour between dendrites in which only fast spiking could be evoked and dendrites in which compound spiking was also seen is not likely to be due to a lack of high-threshold Ca^{2+} channels. Ca^{2+}-dependent spikes could still be evoked in the first group of dendrites under conditions which blocked or reduced I_A, indicating that the density of Ca^{2+} channels is at least high enough to support spike generation. We therefore propose that the dendrites of non-bursting pyramidal neurones are capable of generating both regular fast spiking and compound spiking patterns, but that it is the distribution and density of (principally) I_A in different parts of the dendritic tree that determines which type of response is evoked. Current injection evokes compound spiking, in parts of the dendritic tree in which the density of A-channels is relatively low, and regular fast spikes in areas with a high density of A-channels. One obvious way to test this hypothesis would be to investigate the effect of 4-AP on fast spikes in dendrites in which compound spiking had been blocked by Co^{2+}. We have tried this, but the combination of Co^{2+}-containing medium and 4-AP very rapidly resulted in the appearance of multiple, long-duration bursts which precluded analysis of individual spikes.

Functional implications

The results presented here provide further evidence that Na^{+}- and Ca^{2+}-dependent spikes can be generated locally in the apical dendrites and furthermore indicate that the spike generating capability extends into the distal part of the dendritic tree. The presence of active conductances will have important implications for the electrical properties of the dendrites and therefore on the transformation of synaptic inputs into functionally relevant outputs from the CA1 pyramidal neurones. Theoretical calculations have shown that distal synaptic inputs would be most strongly attenuated (Rall, 1962), thereby contributing much less to somatic depolarization than proximal synapses. However Andersen *et al.* (1980) have shown that proximal and distal synapses are equally efficient in initiating somatic spiking, inferring that there

are active processes in the dendrites. There are several mechanisms by which synaptic amplification can occur. Na^+ and Ca^{2+} channels could work locally as non-linear amplifiers, enhancing the synaptic current. The depolarization produced by this synergistic action will also relieve the voltage-dependent Mg^{2+} block of NMDA receptors (Mayer & Westbrook, 1987), thereby further boosting the synaptic potentials. Finally, the Na^+ and Ca^{2+} channels could generate spikes which propagate to the soma.

The present results suggest that I_A plays an important role in controlling the excitability of the apical dendrites. This would provide a very sensitive and dynamic means of controlling the efficacy of the dendritic tree, maybe even at the level of individual dendritic branches. A reduction in I_A allows enhanced activation of L-type Ca^{2+} channels. This will lead to an increase in the intracellular Ca^{2+} concentration, which in turn regulates other dendritic channels. Depending on the nature of these channels, synaptic potentials could be either amplified or attenuated.

Relatively small changes in $[K^+]_o$ have a striking effect on the firing properties of the apical dendrites and indicates what could happen in the dendritic region under pathophysiological conditions. During epileptic activity, $[K^+]_o$ can increase to 7 mM or more (Fisher *et al.* 1976). It is possible that the resultant increase in dendritic excitability plays an important role in the synchronization and spread of epileptic activity in area CA1 as proposed by Wong & Prince (1979).

The present study, together with the current state of knowledge, shows that dendrites are highly complex structures and that their activity is modulated by both intrinsic and extrinsic mechanisms through which the pyramidal neurones can be tuned to special types of synaptic inputs.

Amitai, Y., Friedman, A., Connors, B. W. & Gutnick, M. J. (1993). Regenerative activity in apical dendrites of pyramidal cells in neocortex. *Cerebral Cortex* **3**, 26–38.

Andersen, P. & Lømo, T. (1966). Mode of activation of hippocampal pyramidal cells by excitatory synapses on dendrites. *Experimental Brain Research* **2**, 247–260.

Andersen, P., Silfvenius, H., Sundberg, S. H. & Sveen, O. (1980). A comparison of distal and proximal dendritic synapses on CA1 pyramids in guinea-pig hippocampal slices *in vitro*. *Journal of Physiology* **307**, 273–299.

Andreasen, M., Lambert, J. D. C. & Jensen, M. S. (1989). Effects of new non-*N*-methyl-D-aspartate antagonists on synaptic transmission in the *in vitro* rat hippocampus. *Journal of Physiology* **414**, 317–336.

Benardo, L. S., Masukawa, L. M. & Prince, D. A. (1982). Electrophysiology of isolated hippocampal pyramidal dendrites. *Journal of Neuroscience* **2**, 1614–1622.

Fisher, R. E., Gray, R. & Johnston, D. (1990). Properties and distribution of single voltage-gated calcium channels in adult hippocampal neurons. *Journal of Neurophysiology* **64**, 91–104.

Fisher, R. S., Pedley, T. A., Moody, W. J. Jr & Prince, D. A. (1976). The role of extracellular potassium in hippocampal epilepsy. *Archives of Neurology* **33**, 76–83.

Fox, A. P., Nowycky, M. C. & Tsien, R. W. (1987). Kinetic and pharmacological properties distinguishing three types of calcium currents in chick sensory neurones. *Journal of Physiology* **394**, 149–172.

Halliwell, J. V. & Adams, P. R. (1982). Voltage-clamp analysis of muscarinic excitation in hippocampal neurons. *Brain Research* **250**, 71–92.

Herreras, O. (1990). Propagating dendritic action potential mediates synaptic transmission in CA1 pyramidal cells in situ. *Journal of Neurophysiology* **64**, 1429–1441.

Jaffe, D. B., Johnston, D., Lasser-Ross, N., Lisman, J. E., Miyakawa, H. & Ross, W. N. (1992). The spread of Na^+ spikes determines the pattern of dendritic Ca^{2+} entry into hippocampal neurons. *Nature* **357**, 244–246.

Jones, O. T., Kunze, D. L. & Angelides, K. J. (1989). Localization and mobility of omega-conotoxin-sensitive Ca^{2+} channels in hippocampal CA1 neurons. *Science* **244**, 1189–1193.

Konnerth, A., Lux, H. D. & Heinemann, U. (1986). Ionic properties of burst generation in hippocampal pyramidal cell somata 'in vitro'. In *Experimental Brain Research*, series 14, *Calcium Electrogenesis and Neuronal Functioning*, ed. Heinemann, U., Klee, M., Neher, E. & Singer, W., pp. 368–374. Springer, Berlin.

Lacaille, J.-C. & Schwartzkroin, P. A. (1988). Stratum lacunosum-moleculare interneurons of hippocampal CA1 region. II. Intrasomatic and intradendritic recordings of local circuit synaptic interactions. *Journal of Neuroscience* **8**, 1411–1424.

Llinás, R. & Sugimori, M. (1980). Electrophysiological properties of *in vitro* Purkinje cell dendrites in mammalian cerebellar slices. *Journal of Physiology* **305**, 197–213.

Masukawa, L. M., Benardo, L. S. & Prince, D. A. (1982). Variations in electrophysiological properties of hippocampal neurons in different subfields. *Brain Research* **242**, 341–344.

Masukawa, L. M. & Prince, D. A. (1984). Synaptic control of excitability in isolated dendrites of hippocampal neurons. *Journal of Neuroscience* **4**, 217–227.

Mayer, M. L. & Westbrook, G. L. (1987). The physiology of excitatory amino acids in the vertebrate central nervous system. *Progress in Neurobiology* **28**, 197–276.

Rall, W. (1962). Theory of physiological properties of dendrites. *Annals of the New York Academy of Sciences* **96**, 1071–1092.

Regan, L. J., Sah, D. W. Y. & Bean, B. P. (1991). Ca^{2+} channels in rat central and peripheral neurons: high-threshold current resistant to dihydropyridine blockers and omega-conotoxin. *Neuron* **6**, 269–280.

Regehr, W. G. & Tank, D. W. (1992). Calcium concentration dynamics produced by synaptic activation of CA1 hippocampal pyramidal cells. *Journal of Neuroscience* **12**, 4202–4223.

Schwartzkroin, P. A. (1975). Characteristics of CA1 neurons recorded intracellularly in the hippocampal in vitro slice preparation. *Brain Research* **85**, 423–436.

Schwartzkroin, P. A. & Slawsky, M. (1977). Probable calcium spikes in hippocampal neurons. *Brain Research* **135**, 157–161.

SEGAL, M. & BARKER, J. L. (1984). Rat hippocampal neurons in culture: potassium conductances. *Journal of Neurophysiology* **51**, 1409–1433.

SHENG, M., TSAUR, M.-L., JAN, Y. N. & JAN, L. Y. (1992). Subcellular segregation of two A-type K^+ channel proteins in rat central neurons. *Neuron* **9**, 271–284.

SOMJEN, G. G. (1979). Extracellular potassium in the mammalian central nervous system. *Annual Review of Physiology* **41**, 159–177.

SPEDDING, M. & PAOLETTI, R. (1992). III. Classification of calcium channels and the sites of action of drugs modifying channel function. *Pharmacological Reviews* **44**, 363–376.

SPENCER, W. A. & KANDEL, E. R. (1961). Electrophysiology of hippocampal neurons. IV. Fast prepotentials. *Journal of Neurophysiology* **24**, 272–285.

STORM, J. F. (1987). Action potential repolarization and a fast after-hyperpolarization in rat hippocampal pyramidal cells. *Journal of Physiology* **385**, 733–759.

STORM, J. F. (1990). Potassium currents in hippocampal pyramidal cells. In *Progress in Brain Research*, vol. 83, *Understanding the Brain Through the Hippocampus*, ed. STORM-MATHISEN, J., ZIMMER, J. & OTTERSEN, O. P., pp. 161–187. Elsevier Science Publishers, Amsterdam.

STUART, G. J. & SAKMANN, B. (1994). Active propagation of somatic action potentials into neocortical pyramidal cell dendrites. *Nature* **367**, 69–72.

TAUBE, J. S. & SCHWARTZKROIN, P. A. (1988*a*). Mechanisms of long-term potentiation: EPSP/spike dissociation, intradendritic recordings and glutamate sensitivity. *Journal of Neuroscience* **8**, 1632–1644.

TAUBE, J. S. & SCHWARTZKROIN, P. A. (1988*b*). Mechanisms of long-term potentiation: a current-source density analysis. *Journal of Neuroscience* **8**, 1645–1655.

TURNER, R. W., MEYERS, D. E. R. & BARKER, J. L. (1989). Localization of tetrodotoxin-sensitive field potentials of CA1 pyramidal cells in the rat hippocampus. *Journal of Neurophysiology* **62**, 1375–1387.

TURNER, R. W., MEYERS, D. E. R., RICHARDSON, T. L. & BARKER, J. L. (1991). The site for initiation of action potential discharge over the somatodendritic axis of rat hippocampal CA1 pyramidal neurons. *Journal of Neuroscience* **11**, 2270–2280.

WESTENBROEK, R. E., AHLIJANIAN, M. K. & CATTERALL, W. A. (1990). Clustering of L-type Ca^{2+} channels at the base of major dendrites in hippocampal pyramidal neurons. *Nature* **347**, 281–284.

WONG, R. K. S. & PRINCE, D. A. (1979). Dendritic mechanisms underlying penicillin-induced epileptiform activity. *Science* **204**, 1228–1231.

WONG, R. K. S. & PRINCE, D. A. (1981). Afterpotential generation in hippocampal pyramidal cells. *Journal of Neurophysiology* **45**, 86–97.

WONG, R. K. S., PRINCE, D. A. & BASBAUM, A. I. (1979). Intradendritic recordings from hippocampal neurons. *Proceedings of the National Academy of Sciences of the USA* **76**, 986–990.

WONG, R. K. S. & STEWART, M. (1992). Different firing patterns generated in dendrites and somata of CA1 pyramidal neurones in guinea-pig hippocampus. *Journal of Physiology* **457**, 675–687.

YAARI, Y., HAMON, B. & LUX, H. D. (1987). Development of two types of calcium channels in cultured mammalian hippocampal neurons. *Science* **235**, 680–682.

Acknowledgements

We would like to thank Dr Jens Christian Sørensen (University of Odense) for doing some of the histochemical work and Tage Honoré (Novo Nordisk) for the gift of CNQX. This work was supported by the Danish Biotechnology Programme, the Danish Medical Research Council and Aarhus Universitets Forskningsfond.

Received 10 February 1994; accepted 22 August 1994.